THE MEASUREMENT OF THE VISCOELASTIC PROPERTIES OF AQUEOUS SOLUTIONS OF POLYETHYLENE OXIDE

By

JOHN RIORDON WYHOF II

Bachelor of Arts

Middlebury College

Middlebury, Vermont

1965

Submitted to the Faculty of the Graduate School
of the Oklahoma State University
in partial fulfillment of the requirements
for the degree of
MASTER OF SCIENCE
May, 1967

THE MEASUREMENT OF THE VISCOELASTIC PROPERTIES OF AQUEOUS SOLUTIONS OF POLYETHYLENE OXIDE

Thesis Approved:

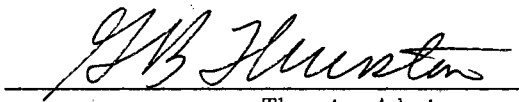

Thesis Adviser

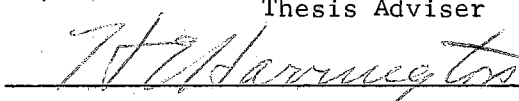

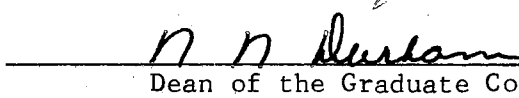

Dean of the Graduate College

ACKNOWLEDGEMENTS

The author would like to take this opportunity to express his appreciation to all those who have assisted him in this investigation: to Dr. G. B. Thurston, for his constant guidance and valuable criticism; to his wife Nancy Lou for her assistance and encouragement; to Mr. and Mrs. John L. Schrag for their help in proofreading the manuscript; and to the Office of Naval Research for the grants awarded to Dr. Thurston which made possible this research.

TABLE OF CONTENTS

LIST OF FIGURES

CHAPTER I

INTRODUCTION

A. The Problem

One means of studying the properties of a high molecular weight polymer is to investigate the viscoelastic properties displayed by a solution resulting from the addition of the polymer to a viscous medium. These properties can be determined by exerting a mechanical shear on the solution and by then determining the change due to the presence of the macromolecules in the solution. Certain characteristics of the polymer can be determined when the results are related to the theoretical models which have been developed. In this investigation polymer solutions of finite concentration were studied using a mechanical shear method. An existing dilute-solution theory was extended to include finite concentrations, and the experimental results obtained were compared to the existing theory.

B. Description of the Polymer

Polyethylene oxide is one of the few high molecular weight molecules soluble in water. The particular structure of the monomer units, $-CH_2-CH_2-O-$, allows this molecule to have this unusual property, and thus to differ from its cousins, polymethylene oxide, $-CH_2-O-$, and polypropylene oxide, $-C_3H_6O-$, which are insoluble in water (1). When polyethylene oxide is dissolved in water, it is known to form long chains of monomer units, resulting in a solution which displays viscous

and elastic properties.

Polyox, a commercial grade polyethylene oxide resin, was developed by the Union Carbide Company. The initial investigation of solutions containing Polyox was made by Bailey, Powell and Smith (2), while Hill, Bailey and Fitzpatrick (3) studied the polymerization process and the production of the resin, using strontium carbonate as a catalyst. The effects upon the intrinsic viscosity by the addition of various salts was shown by Bailey and Callard (1). A comprehensive description of the resin and outline of the industrial uses is given in the manufacturer's advance technical bulletin (4).

Other investigations of the viscous and elastic (5, 6, 7) properties of polyethylene oxide (PEO) have shown the solutions to have a non-Newtonian character and a great viscosity dependence upon the solute concentration. In order to compare results with present "dilute" solution theory (8), it would have been desirable to experiment at such low concentrations that any concentration dependent effects not included in the theory would be negligible. Such a condition was impractical, however, since the solution viscosity would be only 20 per cent greater than that of water, thus making measurement conditions extremely limited.

C. Macromolecular Theories

In attempting to describe the behavior of large molecules in solution, several theoretical models have been developed. In general, the various configurations of the molecules in solution are used to relate the behavior of the microscopic model to the macroscopically observed behavior. The development of a theoretical model consists of first describing all the forces which affect the molecule and then

determining the changes in configuration due to these forces.

The model suggested by Haller (9), Boeder (10), and W. Kuhn (11) consists of rigid rod-like particles dissolved in a fluid medium, dilute enough that there are no interactions between particles. In this model, the rod-like particle would align itself according to the shear forces, while the Brownian motion would tend to randomly orientate the particle. The orientation due to the hydrodynamic field and Brownian motion is described by a distribution function. The function developed by Haller gives the frequency of finding the particle oriented in different directions. In the theory developed by Boeder for colloid particles, the molecule is represented by large ellipsoids of revolution. The distribution function, which considers the same forces as Haller's, describes the orientation of the axes. The model developed by W. Kuhn consists of rigidly connected spheres. A similar function was developed to describe the orientation of the rigid chain about its center of gravity (12). It is apparent that although this model is helpful in describing the optical properties of some macromolecules, many difficulties arise in the description of the viscoelastic properties of flexible molecules.

Haller also suggested the development of a deformable particle to account for the elasticity observed. In the theory of Cerf (13) the macromolecular model, no longer rigid, is represented by an elastic sphere. The sphere is deformed by the velocity gradients into an ellipsoid. The elasticity then attempts to restore the model to a sphere. Cerf proposed that an internal viscosity of the molecule opposes the deformation and restoration. The Brownian motion is depicted as causing fluctuations in the shape of the particle. In the

first approximation, the Brownian motion does not affect the orientation of the particle, as it does for the rigid particle model. In applying this model to chain molecules, Cerf considered the volume of the sphere as that volume occupied by the most probable configuration of the molecule. The surface of the sphere is defined as the limits of the chain and the associated solvent.

In determining the dependence of intrinsic viscosity on molecular weight, Flory (14) suggested a model in which the fluid was locked into an "equivalent hydrodynamic sphere." The frictional coefficient was then determined from Stokes law. This simple model contained a fundamental deficiency: the determination of the "equivalent radius of the sphere."

The chain molecule in solution, as described by Zimm (15), is represented by a long string of "elastic dumbbells" immersed in a viscous medium. Each "elastic dumbbell" represents a polymer segment which is able to pivot about the bead at the ends of the spring. In describing the motion of the chain, when the fluid is sheared, several forces are considered: (1) the force exerted by the viscous medium on the beads; (2) the force exerted on the bead by the springs; (3) Brownian motion; and (4) hydrodynamic interaction effects of one segment upon another. Using normal coordinates, differential equations are set up to relate these forces to the velocity gradient. Since there are many such segments, eigenvalue equations are set up, and the total solution contains summations of these eigenvalues. Although the Zimm theory describes the molecule in greater detail, it is only directly applicable to dilute solutions.

The problem of cross-linking and entanglement coupling which occurs

in concentrated solutions has been studied by Ferry (16). In the models discussed by Ferry the molecular behavior becomes dependent upon the number of cross-links rather than the solvent. For the case of entanglement coupling, where the long chains temporarily become entwined, the viscosity first increases rapidly with increasing molecular weight, but then this increase becomes less rapid as more free ends are available. Ferry suggests the use of an effective friction coefficient to account for the entanglement when it occurs.

D. Empirical Studies

In order to keep the simple molecular model, several empirical attempts have been made to reduce the oscillatory shear data obtained from concentrated solutions, so that the interaction effects can be included. In studying a polyisobutylene-Decalin system, Dewitt, Markovitz, Padden, and Zapas (17) suggested the use of a c^2 reduction, where c is the solution concentration. It was suggested that a temporary gel structure was present due to molecular coupling. In the investigation of concentrated solutions of polystyrene and polyisobutylene, Ferry (18) demonstrated the use of a simple c reduction.

Empirical relations were also suggested to describe the dependence of steady flow viscosity on shear rate for concentrated solutions. Many of these relationships are compared by Rodriguez (6) in the investigation of polyethylene oxide and other chain molecules. Experimental relationships have also been developed to relate the intrinsic viscosity to the specific or relative viscosity for concentrated solutions.

In extending the viscosity for infinitely dilute solutions, Peterlin (19) introduced an "effective solvent viscosity" to account

for the presence of the other molecules when the solutions had finite concentrations. Thus the expression for an infinitely dilute solution,

$$\eta = \eta_s + \eta_s[\eta]c \tag{I-1}$$

will become

$$\eta = \eta_s + \eta^*[\eta]c \tag{I-2}$$

for solutions of finite concentration where η^* is the "effective solution viscosity."

CHAPTER II

THEORY

A. The Kirkwood-Riseman Method for Obtaining the Intrinsic Viscosity

In the study of macromolecules in solution, it is first necessary to relate the changes in solution properties due to the addition of the polymer to a microscopic model. It is therefore necessary to choose a model which has characteristics like the polymer under investigation. The chemical structure of polyethylene oxide suggests a model represented by a segmented chain.

The theory developed by Kirkwood and Riseman (20) is an improvement on the theory of Kuhn (11), Huggins (21) and Kramers (22) since the hydrodynamic interaction between the chain segments is considered. When considering this interaction, it is realized that the outer chain elements not only affect the motions of the other segments, but may also shield the motion of the fluid from the inner segments. The theory of Kuhn, Huggins and Kramers neglects this segment interaction, and considers each segment to have the same resistance to the fluid as when no other polymer segments are there.

The Kirkwood-Riseman theory employs a more realistic model, the random coil, consisting of n segment elements. The chain is suspended in a fluid medium, which has a velocity $\vec{V}_o(\vec{R})$ in the $+X$ direction. Since a velocity gradient exists in the laminar flow field, the magnitude of the velocity will depend on the y component

of R . If the ℓ^{th} chain segment is considered, then $\vec{V}_\ell$ is the velocity the fluid would have, if the segment were not at that point, and $\mathcal{U}_\ell$ is the velocity of the segment. Then the force exerted by the chain segment on the fluid is given by

$$\vec{\vec{F}}_\ell = \mathcal{f}(\vec{V}_\ell - \vec{\mathcal{U}}_\ell) \tag{II-1}$$

where $\mathcal{f}$ is the friction constant for the fluid.

From the formula developed by Oseen (23) the perturbation velocity V' at location $\vec{R}_\ell$, where the center of mass of the coil is located at $x = 0$, $y = 0$, $z = 0$, is given by

$$\vec{V}'(\vec{R}_\ell) = \vec{\vec{T}}(\vec{R}_\ell) \cdot \vec{\vec{F}}_\ell \tag{II-2}$$

where $\vec{\vec{T}}(\vec{R}_\ell)$ is the segmental interaction tensor. The perturbation effect developed here gives the perturbation velocity at the position of segment ℓ due to the forces exerted by the other elements on the fluid. It should be noted that the hydrodynamic forces due to other chains on the ℓ^{th} segment are not considered. The formulation developed by Oseen and used here by Kirkwood and Riseman is applicable to very dilute solutions.

The total fluid velocity V_ℓ° at the location of element ℓ consists of the unperturbed velocity at that element plus the summation of the perturbed velocities due to the other elements. If the summation is performed for S elements, then

$$\vec{V}_\ell = \vec{V}_\ell^\circ - \int \sum_{S=-n}^{+n} \vec{\vec{T}}_{\ell s} \cdot (\vec{V}_s - \vec{\mathcal{U}}_s) \qquad (n \neq \ell) \tag{II-3}$$

where R_{ls} is the distance between elements l and s, and the interaction tensor is given by

$$\vec{\vec{T}}_{ls} = (1/8\pi\eta_o R_{ls})\{1 + \vec{R}_{ls}\vec{R}_{ls}/R_{ls}^2\}. \tag{II-4}$$

Substituting for $\vec{V}_l$ in equation (II-1), the forces exerted by the chain elements on element l are given by

$$\vec{F}_l = -\zeta(\vec{V}_l^{\,o} - \vec{u}_l) - \zeta \sum_{s=-n}^{+n} \vec{\vec{T}}_{ls} \cdot \vec{F}_s \quad (n \neq l) \tag{II-5}$$

Now the forces due to the polymer coil in a viscous medium on the boundaries of the medium will be considered. According to the method developed by Oseen, the polymer is placed in a fluid in laminar flow. The flow is in the $+x$ direction between two parallel plane boundaries, of infinite extent, located at $y = +h_2$ and $y = -h_1$. The coordinate axes are centered on the center of mass of the polymer chain. The polymer, being in equilibrium, has a mean velocity equal to that of the fluid velocity surrounding it. For such a condition the mean internal and external angular velocity must have values such that the average torques are zero.

The unperturbed velocity of element l is given by

$$\vec{V}_l^{\,o} = \dot{\epsilon}\,(\vec{R}_{ol} \cdot \vec{e}_y)\vec{e}_x \tag{II-6}$$

where $\vec{e}_x$, $\vec{e}_y$, and $\vec{e}_z$ are the unit vectors for the coordinate system, $\dot{\epsilon}$ is the rate of strain and $\vec{R}_{ol}$ is the distance of the l^{th} element from the center of mass. In order to eliminate any external average torque due to viscous drag, the value of the average angular velocity must be $\dot{\epsilon}/2$ in the $-z$ direction. This can readily

be seen if the average polymer configuration is imagined as a sphere with slight fluctuations. The fluctuations existing for the actual polymer are neglected in the consideration of the angular velocities and only an average is used. In vector notation the velocity of the ℓ^{th} element of the chain is given by

$$\vec{u}_\ell = -\dot{\epsilon}/2\,(\vec{e}_x \times \vec{R}_{o\ell}) \,. \tag{II-7}$$

Then expanding the velocity,

$$\vec{u}_\ell = -(\dot{\epsilon}/2) \begin{vmatrix} i & j & k \\ 0 & 0 & 1 \\ R_{o\ell_x} & R_{o\ell_y} & R_{o\ell_z} \end{vmatrix} \tag{II-8}$$

and

$$\vec{u}_\ell = -(\dot{\epsilon}/2)\left[(R_{o\ell_x})\vec{j} - (R_{o\ell_y})\vec{i}\right] . \tag{II-9}$$

But $R_{o\ell_x} = \vec{R}_{o\ell}\cdot\vec{e}_x$ and $R_{o\ell_y} = \vec{R}_{o\ell}\cdot\vec{e}_y$. Then the velocity is given by

$$\vec{u}_\ell = (\dot{\epsilon}/2)\left[(\vec{R}_{o\ell}\cdot\vec{e}_y)\vec{e}_x - (\vec{R}_{o\ell}\cdot\vec{e}_x)\vec{e}_y\right] \tag{II-10}$$

since $\vec{j} = \vec{e}_y$ and $\vec{i} = \vec{e}_x$.

Substituting for $\vec{V}_\ell^{\circ}$ and $\vec{u}_\ell$ in equation (II-5), then the forces exerted by the ℓ^{th} segment on the fluid at location ℓ are given by

$$\vec{F}_\ell = -\zeta\left[\dot{\epsilon}\,(\vec{R}_{o\ell}\cdot\vec{e}_y)\vec{e}_x - \{\tfrac{\dot{\epsilon}}{2}(\vec{R}_{o\ell}\cdot\vec{e}_y)\vec{e}_x - \tfrac{\dot{\epsilon}}{2}(\vec{R}_{o\ell}\cdot\vec{e}_x)\vec{e}_y\}\right]$$

$$-\zeta\sum_{s=-n}^{n}\vec{T}_{\ell s}\cdot\vec{F}_s$$

$$\vec{\vec{F}}_\ell = -\frac{\rho\dot{\epsilon}}{2}\left[2(\vec{R}_{o\ell}\cdot\vec{e}_y)\vec{e}_x - (\vec{R}_{o\ell}\cdot\vec{e}_y)\vec{e}_x + (\vec{R}_{o\ell}\cdot\vec{e}_x)\vec{e}_y\right] - \int\sum_{s=-n}^{+n}\vec{\vec{T}}_{\ell s}\cdot\vec{\vec{F}}_s$$

$$= -\frac{\rho\dot{\epsilon}}{2}\left[(\vec{R}_{o\ell}\cdot\vec{e}_y)\vec{e}_x + (\vec{R}_{o\ell}\cdot\vec{e}_x)\vec{e}_y\right] - \int\sum_{s=-n}^{+n}\vec{\vec{T}}_{\ell s}\cdot\vec{\vec{F}}_s \cdot \tag{II-11}$$

Again from Oseen's formula, the perturbation in flow due to the molecule as a whole at a point R from the center of mass of the molecule is given by

$$\vec{V}'(\vec{R}) = \frac{1}{8\pi\eta_o}\sum\left\{\frac{F_\ell}{|R-R_{o\ell}|} + \frac{(R-R_{o\ell})(R-R_{o\ell})\cdot F_\ell}{|R-R_{o\ell}|^3}\right\}. \tag{II-12}$$

In the simplification of Oseen's formula, this equation was obtained if R was assumed large. The equation obtained for the perturbations due to other segments assumed that R was small. The velocity was expanded in spherical harmonics and averaged over all internal configurations. Then for distances which are large compared to chain dimensions the average perturbation velocity at location $\vec{R}$ is given by

$$\langle V'\rangle_{Av} = \frac{-3\rho G\dot{\epsilon}}{4\pi\eta_o R^5}(\vec{R}\cdot\vec{e}_x)(\vec{R}\cdot\vec{e}_y)\vec{R} \tag{II-13}$$

where

$$G = \frac{1}{\rho\dot{\epsilon}}\sum_{\ell=-n}^{+n}\left\langle(\vec{F}_\ell\cdot\vec{e}_x)(\vec{R}_{o\ell}\cdot\vec{e}_y)\right\rangle_{Av}. \tag{II-14}$$

The method developed by Burgers (23) is now used to sum the contributions $\langle \vec{v}' \rangle_{Av}$ at the parallel boundaries. Writing the components of $\langle \vec{v}' \rangle_{Av}$ in terms of the coordinates previously defined

$$\langle a \rangle_{Av} = \frac{-3\rho G \dot{\epsilon}}{4\pi\eta_0} \cdot \frac{x^2 y}{(x^2+y^2+z^2)^{5/2}}$$

$$\langle b \rangle_{Av} = \frac{-3\rho G \dot{\epsilon}}{4\pi\eta_0} \cdot \frac{y^2 x}{(x^2+y^2+z^2)^{5/2}}$$

$$\langle c \rangle_{Av} = \frac{-3\rho G \dot{\epsilon}}{4\pi\eta_0} \cdot \frac{xyz}{(x^2+y^2+z^2)^{5/2}} \qquad \text{(II-15)}$$

where

$$\langle \vec{v}' \rangle_{Av} = \langle a \rangle_{Av} \vec{i} + \langle b \rangle_{Av} \vec{j} + \langle c \rangle_{Av} \vec{k}$$

the summation can be accomplished by integrating over the infinite plane boundary. Then for the contributions in the x direction,

$$\langle a \rangle_{Av} = \frac{-3\rho G \dot{\epsilon}}{4\pi\eta_0} \int_{-\infty}^{\infty}\int_{-\infty}^{\infty} \frac{x^2 y \, dx\, dz}{(x^2+y^2+z^2)^{5/2}} \cdot$$

(II-16)

Using the trignometric substitution,

$$x = a \tan u \,, \quad dx = a \sec^2 u \, du$$

(II-17)

where $a^2 = y^2 + z^2$. Then changing to the proper limits,

when $x = -\infty$, $u = -\pi/2$

and when $x = \infty$, $u = \pi/2$

and carrying out the first integration,

$$\langle a \rangle_{Av} = \frac{-3\varsigma G\dot{\epsilon}}{4\pi\eta_0} y \int_{-\infty}^{\infty}\int_{-\pi/2}^{\pi/2} \frac{a^2 \tan^2 u \cdot a\sec^2 u \, du\, dz}{(a^2\tan^2 u + a^2)^{5/2}}$$

$$= \frac{-3\varsigma G\dot{\epsilon}}{4\pi\eta_0} y \int_{-\infty}^{\infty}\int_{-\pi/2}^{\pi/2} \frac{\sin^2 u \cdot \cos u \, du\, dz}{a^2}$$

$$= \frac{-3\varsigma G\dot{\epsilon}}{4\pi\eta_0} y \int_{-\infty}^{\infty} \frac{\sin u}{3a^2} \Bigg]_{-\frac{\pi}{2}}^{\frac{\pi}{2}} dz$$

$$= \frac{-3\varsigma G\dot{\epsilon}}{4\pi\eta_0} y \int_{-\infty}^{\infty} \frac{2\, dz}{3(y^2+z^2)} \quad .$$

(II-18)

Now integrating with respect to z, using trignometric substitutions, where

$$z = y \tan u$$
$$dz = y \sec^2 u \, du \qquad \text{(II-19)}$$

and changing the limits, such that

when $\quad x = -\infty \, , \; u = -\pi/2$

and $\quad x = \infty \, , \; u = \pi/2$

then

$$\langle a \rangle_{Av} = \frac{-\varsigma G\dot{\epsilon}}{2\pi\eta_0} y \int_{-\frac{\pi}{2}}^{\frac{\pi}{2}} \frac{y\sec^2 u \, du}{(y^2 + y^2\tan^2 u)}$$

$$= \frac{-\rho G \dot{\epsilon}}{2\pi\eta_o}\left[\pi/2 - (-\pi/2)\right]$$

$$= \frac{-\rho G \dot{\epsilon}}{2\eta_o} \quad . \tag{II-20}$$

Carrying out the integrations in a similar manner for the perturbation velocity components in the y and z directions yielded

$$\langle b \rangle_{AV} = 0 \quad , \quad \langle c \rangle_{AV} = 0 \quad . \tag{II-21}$$

Therefore from equation (II-15) the total velocity is given by

$$\langle \vec{v}' \rangle_{AV} = \frac{-\rho G \dot{\epsilon}}{2\eta_o} \quad . \tag{II-22}$$

This result shows that there are no average perturbations at the plane in the y and z directions. Integrating over both planes, $y = -h_1$ and $y = +h_2$, the total perturbation velocity difference due to one chain is given by $-\rho G \dot{\epsilon}/\eta_o$. If there are n chains per unit volume between the two planes, then the total number of chains is given by

$$N = n\,(h_2 + h_1)\cdot A \tag{II-23}$$

where A is the area of a plane. And the mean rate of shear between the two planes is

$$\dot{\epsilon}_p = \frac{N\,(-\rho G \dot{\epsilon}/\eta_o)}{(h_2 + h_1)\cdot A}$$

$$\dot{\epsilon}_p = \frac{-\rho G \dot{\epsilon} n}{\eta_o} \quad . \tag{II-24}$$

Then the total effective mean rate of shear between the two planes will be given by

$$\dot{\epsilon}_{eff} = \dot{\epsilon} + \dot{\epsilon}_p$$
$$= \dot{\epsilon}\left(1 - \frac{\rho G n}{\eta_o}\right) . \qquad \text{(II-25)}$$

Since the average stress τ over any plane parallel to the field of flow will remain constant, the effective viscosity is given by

$$\eta_{eff} = \frac{\tau}{\dot{\epsilon}_{eff}} , \quad \tau = \eta_o \dot{\epsilon} . \qquad \text{(II-26)}$$

Then substituting equation (II-25) into equation (II-26),

$$\eta_{eff} = \frac{\dot{\epsilon}\eta_o}{\dot{\epsilon}\left(1 + \frac{\rho G n}{\eta_o}\right)} . \qquad \text{(II-27)}$$

Since the value of $\rho G n / \eta_o$ has been assumed small, the higher order terms can be neglected in the expansion and the effective viscosity will be given by

$$\eta_{eff} = \eta_o\left(1 + \frac{\rho G n}{\eta_o}\right)$$
$$= \eta_o + \rho G n . \qquad \text{(II-28)}$$

The number of chains per unit volume n is given by

$$n = \frac{N_a c}{M} \qquad \text{(II-29)}$$

where N_a is Avagadro's number, M is the molecular weight of the chain and c is the concentration with units of gm/cc. The intrinsic viscosity $[\eta]$ is defined as

$$[\eta] = \lim_{c \to 0} \frac{\eta_{eff} - \eta_o}{\eta_o c} \quad . \tag{II-30}$$

Since the theory has already assumed the limiting value of the concentration, the value of the intrinsic viscosity is

$$[\eta] = \frac{\rho G N_a}{M \eta_o} \tag{II-31}$$

where the intrinsic viscosity has units of cc/gm. Substituting the expression for G in the corrected form (25) into equation (II-31), then

$$[\eta] = \frac{N_a}{M \eta_o \dot{\epsilon}} \sum_{l=-n}^{+n} \left\langle (\vec{F}_l \cdot \vec{e}_x)(\vec{R}_{ol} \cdot \vec{e}_y) \right\rangle_{Av} \quad . \tag{II-32}$$

Since $(\vec{F}_l \cdot \vec{e}_x) = F_{lx}$, and $(\vec{R}_{ol} \cdot \vec{e}_y) = y_l$, equation (II-32) becomes

$$[\eta] = \frac{N_a}{M \eta_o \dot{\epsilon}} \sum_{l=-n}^{+n} \left\langle F_{lx} \cdot y_l \right\rangle_{Av} \quad . \tag{II-33}$$

As the sum of the averages is equal to the average of the sum, this expression can be written in the form used by Zimm. In his theory, the flow field is in the $+x$ direction and the gradient is in the $+y$ direction. Then changing coordinates, the intrinsic viscosity, as used by Zimm, is

$$[\eta] = \frac{N_a}{M \eta_o \dot{\epsilon}} \left\langle \sum_{l=-n}^{+n} z_l \cdot F_{xl} \right\rangle_{Av} \quad . \tag{II-34}$$

In the derivation of this expression many assumptions and restrictions have been made. The approximations used in Oseen's

interaction formula assume that the forces and motions are quasi-static. This restricts the expression obtained to small gradients. Since oscillatory motion is not discussed in Burger's development, there will likely be some restrictions for this type of motion also. Some question as to the validity of the final expression may be raised, since Oseen's expressions for the perturbations due to the chain assume the chain dimensions to be small compared to R, the distance to the plane. Burgers then determines the number of particles to be summed, by filling the entire space between the planes with particles. The expressions previously derived would not apply to these chains. Of course, it can be assumed that most of the chains are not located near the planes. But within these restrictions, equation (II-32) gives a basic relationship between a microscopic model and the observed viscosities.

B. The Zimm Theory

Considering the linear configuration of the polyethylene oxide molecule in solution, the Zimm (8) model offers the most reasonable comparison for dilute solutions. Unlike the representation of Kirkwood and Riseman, Zimm's model consists of N spring-like segments joining $N+1$ beads. All forces considered act on these beads which form freely rotating joints between the spring-like segments. In the model used by Kirkwood and Riseman, there are N flexible segments represented by equivalent hydrodynamic spheres on which the forces acted. Zimm assumes each segment to have a gaussian probability for the distribution of the components of length. The fluctuations of the segments, each of equal length b, will cause the chain to assume all

possible configurations (25). Neglecting the fact that one segment cannot occupy the same space as another, the most probable configuration can be considered statistically. The resulting gaussian distribution is analagous to random walk distribution. This distribution represents the quiescent configuration of the springs between the beads.

To simplify the notation in developing the forces applied to the beads, a single "elastic dumbbell" segment can be considered and results can be qualitatively applied to the whole chain. If the segment is placed in a viscous medium, the viscous drag exerted on one of the beads is given by the product of the bead velocity and the resistance coefficient. The force exerted by the spring between the beads is given by a spring constant times the displacement between the beads. Then for the one-dimensional case, the forces are related by

$$\rho \dot{x}_1 = F_{x_1} = -g(x_1 - x_2)$$
$$\rho \dot{x}_2 = F_{x_2} = -g(x_2 - x_1) \qquad \text{(II-35)}$$

where x_1 and x_2 are the bead coordinates and ρ is the resistance coefficient. The spring constant g, given by

$$g = 3kT/b^2 \qquad \text{(II-36)}$$

where k is Boltzmann's constant and T is the absolute temperature, allows the force exerted by the spring to obey Hooke's law. The dependence on temperature and segment length indicates the dependence upon the distribution associated with each segment. If the temperature and thus random motion are increased, a greater force will be

necessary to change the configuration of the segment.

The thermal agitation or Brownian motion must also be considered. A probability distribution function ψ is defined, to give the spatial location of the $N+1$ beads of the chain. When considering the chain, this function gives the probability of finding the bead between x and $x+dx$. According to the theory of Brownian motion, the force on the bead is given by

$$-kT\frac{\partial \ln \psi}{\partial x} \tag{II-37}$$

where k is Boltzmann's constant and T is the absolute temperature. The distribution function associated with the Brownian motion represents diffusion according to Fick's law. A current flows from a region of high concentration to one of lower concentration. This flow is proportional to the difference in concentrations times the value of kT. These forces are now included in the Kirkwood-Riseman approximation of Oseen's interaction formula, which describes the effects of these forces on the motion of the fluid. Vector and matrix notations are now used to derive the differential equation of diffusion. It is also necessary to consider the changes in flow motion near the chain caused by the motion of the chain itself. If the flow can be approximated as laminar flow between two liquid planes, this hydrodynamic interaction is treated, using the same method developed by Burgers for intrinsic viscosity.

If oscillatory or steady shear forces are introduced into the system, then the relaxation times of the molecules can be determined. At low frequency or low steady flow gradients the true solution viscosity is observed, since the molecule is rotated with the flow

gradient. The energy imparted to the molecule is allowed time to return through gradual dissipation to the fluid, and energy is lost. At high frequencies, the molecules, which have a spring-like character, absorb energy upon extension during one phase, but do not have time to dissipate the stored energy. When the motion is reversed the stored energy is returned to the fluid and there is little loss of energy, resulting in a small viscosity.

In general, flexible molecules of the type studied here exhibit a viscous character at low frequencies and an almost completely elastic character at high frequencies. At frequencies between these extremes, both elastic and viscous characteristics are observed.

C. Extension of the Zimm Theory

The results of the Zimm theory have been given by Thurston and Schrag (26) emphasizing the finite character of the number of chain segments. From the result,

$$\frac{\eta^* - \eta_s}{\eta_0 - \eta_s} = \frac{\sum_{p=1}^{N} \frac{(\tau_p/\tau_1)}{1 + i\omega\tau_1(\tau_p/\tau_1)}}{\sum_{p=1}^{N} (\tau_p/\tau_1)} \qquad \text{(II-38)}$$

where η^* is the complex viscosity, η_s is the solvent viscosity, η_0 is the steady flow viscosity, ω is the angular frequency, τ_p is a relaxation time, and N is the number of segments. The reduction function a is defined by

$$\tau_1 = a\tau_{1R} \qquad \text{(II-39)}$$

where τ_{1R} is a reference relaxation time.

If equation (II-39) is substituted into equation (II-38), then

$$\frac{\eta^* - \eta_s}{\eta_0 - \eta_s} = \frac{\sum_{P=1}^{N} \frac{(\tau_P/\tau_1)}{1 + i\omega a \tau_{1R} (\tau_P/\tau_1)}}{\sum_{P=1}^{N} (\tau_P/\tau_1)} . \qquad \text{(II-40)}$$

From the nature of equation (II-38), $(\eta^* - \eta_s)/(\eta_0 - \eta_s)$ is a function of $\omega\tau_1$, while in equation (II-40) $(\eta^* - \eta_s)/(\eta_0 - \eta_s)$ is a function of $\omega a \tau_{1R}$. Then using the reduction function a, the resulting curve has the same shape as the unreduced curve, but is shifted along the $a\omega$ axis by the value of τ_{1R}.

The function a, defined by equation (II-39), can be determined from the relationship between τ_1 and the considered parameters.

Since it is not possible to determine the viscoelastic properties of polyethylene oxide under the conditions required by the Zimm theory, a reduction scheme is needed to reduce the finite concentration data in such a manner that it can be extrapolated to give the values of constants normally derived from dilute solution data.

In using the results of the Zimm theory, it should be noted that the segment length ℓ is independent of the other parameters discussed. The extension of the theory to concentrated solutions is based on the assumption that the friction factor f is not only a function of temperature, but also of concentration. Then from the results of the Zimm theory, the first relaxation time is given by

$$\tau_1 = \frac{\ell^2 f}{6kT\lambda_1} \qquad \text{(II-41)}$$

where λ_1 is the first eigenvalue, T is the absolute temperature and k is Boltzmann's constant. If the temperature and molecular

weight are held constant, then, since τ_1 can be expressed as a function of intrinsic viscosity (27),

$$\tau_1 = \frac{[\eta]_o M \eta_s C}{N_a k T} \tag{II-42}$$

where $[\eta]_o$ is the intrinsic viscosity, η_s is the solvent viscosity, and C is a function of M and the hydrodynamic interaction. For constant molecular weight and temperature the hydrodynamic interaction is assumed to be nearly constant. Then

$$a_c = \frac{\tau_1}{\tau_{1R}} = \frac{[\eta]_o \eta_s}{[\eta]_{oR} \eta_{sR}} \cdot \tag{II-43}$$

A constant k particular to a solution is defined as

$$k[\eta]_o = \frac{\eta_o - \eta_s}{\eta_s c} \tag{II-44}$$

where the value of k is 1 for an infinitely dilute solution. Extending equation (II-43) to finite concentrations,

$$a_c = \frac{\frac{\eta_o - \eta_s}{c}}{\left(\frac{\eta_o - \eta_s}{c}\right)_R} = \frac{k[\eta]_o \eta_s}{k_R [\eta]_{oR} \eta_{sR}} \cdot \tag{II-45}$$

Since the molecular weight and temperature are constant, η_s and $[\eta]_o$ are also constant. Then equation (II-45) becomes

$$a_c = \frac{k}{k_R} \cdot \tag{II-46}$$

If the concentration and molecular weight are constant, then a function a_T can be defined as

$$a_T = \frac{\tau_1}{\tau_{1R}} = \frac{T_R}{T} \cdot \frac{(\eta_o - \eta_s)}{(\eta_o - \eta_s)_R} \quad \text{(II-47)}$$

For the concentration and temperature constant a function a_M can be defined as

$$a_M = \frac{\lambda_{1R}}{\lambda_1} = \frac{\tau_1}{\tau_{1R}} \quad \text{(II-48)}$$

It has been shown that if N is large (27)

$$\lambda_1 \simeq \frac{\pi^2}{N^2} + 17.724 h^* N^{-3/2} \quad \text{(II-49)}$$

If the hydrodynamic interaction factor h^* is not small, then equation (II-49) becomes

$$\lambda_1 \simeq (\text{constant}) N^{-3/2} \quad \text{(II- 50)}$$

But since $M \propto N$, then

$$\lambda_1 \simeq (\text{constant}) M^{-3/2} \quad \text{(II-51)}$$

If h^* is small, then λ_1 is related to M by

$$\lambda_1 \simeq (\text{constant}) M^{-2} \quad \text{(II-52)}$$

The relationship between intrinsic viscosity and molecular weight is given by

$$[\eta]_o = (\text{constant}) M^p \quad \text{(II-53)}$$

It has been shown (27) for the free-draining model that $p = 1$ and h^* is small, and for the non-free-draining model that $p = .5$ and h^* is large. For the one limiting case where h^* is not

small, equation (II-53) can be substituted into equation (II-51) and the value of λ_1 becomes

$$\lambda_1 \simeq (\text{constant}) \frac{M^{-1}}{[\eta]_o}$$

$$\simeq (\text{constant}) \frac{1}{M[\eta]_o} . \qquad \text{(II-54)}$$

For the other limiting case where $p = 1$ and h^* is small, equation (II-49) can be substituted into equation (II-53) and

$$\lambda_1 \simeq (\text{constant}) \frac{1}{M[\eta]_o} . \qquad \text{(II-55)}$$

If p and h^* vary in a counterbalancing fashion, then equation (II-55) will hold for all values of h^* and p. The function can then be expressed in measurable quantities. Then, if only the molecular weight is changed,

$$a_M = \frac{\tau_1}{\tau_{1R}} = \frac{M[\eta]}{M_R[\eta]_{oR}} . \qquad \text{(II-56)}$$

Thus, data obtained for a particular molecular weight and temperature can be reduced according to the a_c function given in equation (II-46). And, using the a_M function defined by equation (II-56), data obtained for a particular temperature and k value can be reduced.

CHAPTER III

METHOD OF EXPERIMENT

A. Preparation of Solutions

In preparing dilute solutions of polyethylene oxide, it was desired first, that the solution be clear so that light scattering would not interfere with the optical measurements, and second, that the solution be stable in its viscoelastic properties. One of the more satisfactory methods of preparing small quantities (100 ml) was the "boiling water" technique, as described in the manufacturer's technical bulletin (4).

Deionized water was used to prevent the precipitation of salts which might have formed by the association of free radicals in tap water with the impurities in the commercial grade PEO. Such salts in solution would decrease the viscosity and thus change the properties under investigation (3).

After a measured quantity of water was brought to a boil, the Polyox powder was slowly added, while the water was moderately agitated by a magnetic stirrer. The proportion of powder to water depended on the impurities which would later be removed. This allowance ranged from 10 to 20 per cent above the calculated amount, depending on the manufacturing process of the raw powder. Polyox is insoluble in boiling water; adding it to water of this temperature permitted complete dispersion of the powder, which dissolved as the solution was cooled.

At this preliminary stage the solution was cloudy in appearance. As this would interfere with optical measurements, it was necessary to remove the suspended particles. When the concentration of the solution was low (less than 0.5 per cent), this could be accomplished by dialyzing. As this method was time-consuming, and effective only with low concentrations, centrifugation was found to be more practical. Most solutions were sufficiently cleared when subjected to a force of 15,000 x g for one or two hours, depending on the viscosity of the solution. While this was usually adequate for shear wave propagation, greater clarity was needed for birefringence measurements. This could be attained by passing the solution through a 14 mμ filter.

Hydration and autoxidation can cause unstable solutions. The addition of isopropyl alcohol tends to reduce this problem, since the alcohol competes with the PEO for the peroxides and free radicals (19). A 4:1 ratio of alcohol to resin appeared to adequately stabilize the solution for a period of six weeks. It is known that the addition of alcohol increases the viscosity of the solution, but this change is not appreciable for the amounts used here.

The solute concentration was determined by evaporating the solvent from a measured quantity of solution and determining the weight of the residue. Solutions prepared ranged from 0.5 per cent to 11 per cent, for molecular weights ranging from 4×10^6 to $.064 \times 10^6$. High concentrations were possible only for the lower molecular weights, as the required clarity could not be obtained for the higher molecular weights and high concentrations.

As polyethylene oxide lacked sufficient birefringence for shear wave propagation measurements, it was necessary to add a substance

which possessed this property and at the same time did not appreciably alter the mechanical properties of the original solution. Baymal, a commercial colloidal alumina developed by DuPont, was selected for this purpose. When dispersed in water, Baymal is strongly birefringent. Previous investigations have shown that a dilute (0.3 per cent) Baymal in water solution exhibited approximately the same viscoelastic properties as water alone (29). Thus Baymal would function as an optical indicator, reflecting the mechanical properties of the PEO molecules in solution.

A three per cent water solution of Baymal was prepared using nitric acid as described in the manufacturer's technical report (30). This method was recommended as providing maximum clarity to the sol. The Baymal solution was then added to the Polyox solution to achieve a final Baymal concentration of .15 per cent. In some cases, where more optical sensitivity was desired, the Baymal concentration was increased to .30 per cent. It was observed that when the Baymal was mixed with the Polyox solution small gas bubbles appeared, indicating some chemical reaction was occurring. As this was also found to occur between Baymal and isopropanol alone, it was assumed that the Baymal did not react chemically with the Polyox. The bubbles appeared only at the time of mixing the two solutions, and did not interfere with the measurements.

B. Shear Wave Propagation Measurements

A simplified diagram of the optical arrangement is shown in Figure 1. The system was mounted on a Spindler and Hoyer optical bench supported by a steel mass at the center and smaller masses at the ends. The light source S located at one end was a Helium-Neon gas

Figure 1. Diagram of the Optical System of the Shear Wave Propagation System Showing the Laser Light Source S, Microscope Objective Lens L1, Lens L2, Beam Shifter BS, Polarizer P, Quarter-wave Plate Z, Fluid Cell C, Analyzer A, Diffuser D and Photomultiplier PM.

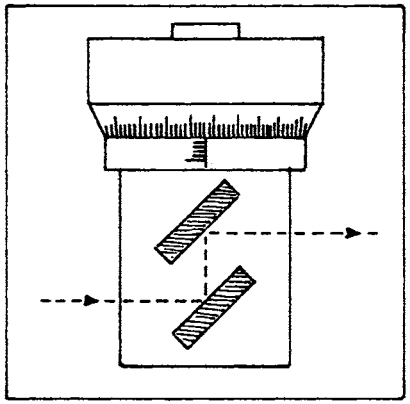

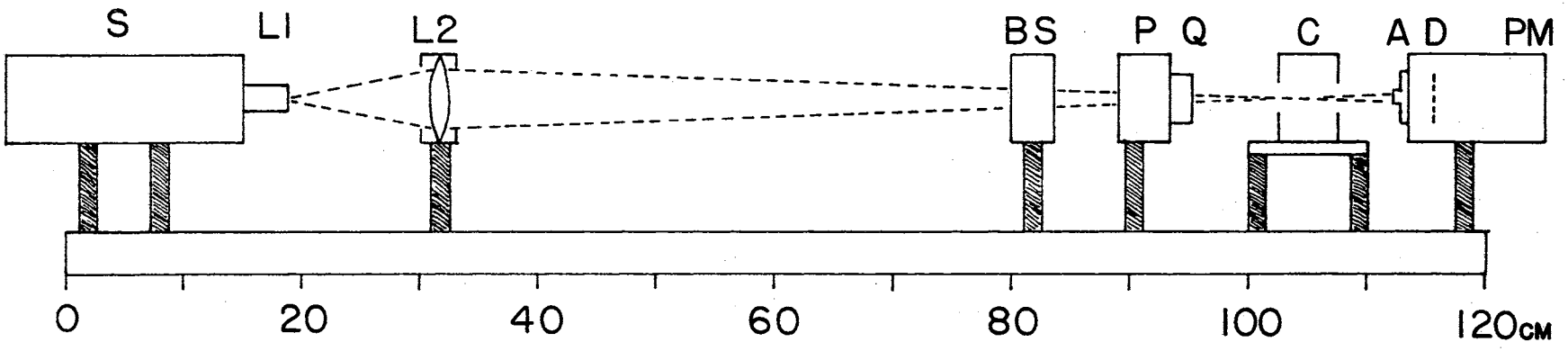
S
LI
L2
BS
P
Q
C
A
D
PM
0
20
40
60
80
100
120CM

laser (EOA's LAS-101). It has an operating wavelength of 6,328 Å and beam width of 2.5 mm. A diverging lens L1 was at the output aperture. A converging lens L2 (100 mm Kodak Ektar) was placed so that the beam would converge at the center of the cell C. Placed along the converging beam's path was a beam shifter, BS. It consisted of two mirrors, one movable, which were set 45° to the beam path, as shown in the inset of Figure 1. By adjusting the micrometer the beam could be moved across the propagation field, permitting observation at any point. The beam then passed through a Glan Thompson polarizer P and a quarter wave plate Q. The light beam, focused at the center of the cell, was right circularly polarized. From the cell the beam passed through another Glan Thompson prism, the analyzer A, which was mounted on the photomultiplier housing. In front of the photomultiplier tube was a diffuser D.

A block diagram of the equipment is shown in Figure 2. The shearing plane was driven by a sinusoidal signal which had originated in an HP Model 2000 oscillator and been passed through a MacIntosh 75-watt amplifier. This amplifier powered the electrodynamic drive coil located at the top of the drive shaft. At this point the current was monitored by an a.c. voltmeter, and was fused to prevent excess current in the drive coil. The velocity of the shaft was monitored with an electrodynamic pickup located below the drive coil on the shaft, and this signal served as a reference for the phase meter. The d.c. component of the photomultiplier output was monitored on a d.c. voltmeter, while the magnitude of the a.c. component was observed with a Hewlett-Packard wave analyzer, Model 302A. The difference in phase of the reference signal and the photomultiplier output signal was measured on

Figure 2. Block Diagram Showing the Electrical Instruments Used with the Shear Wave Propagation System.

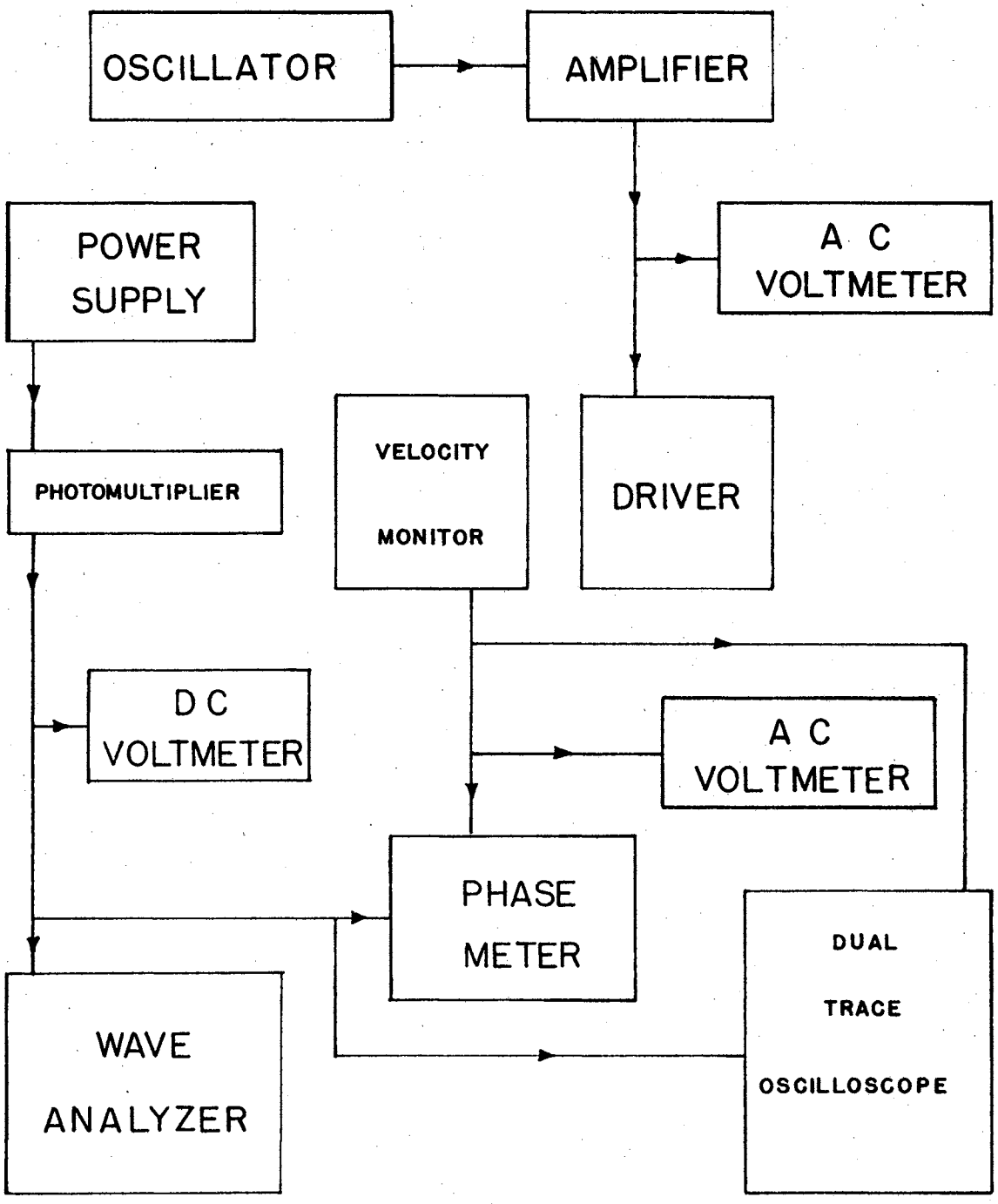
OSCILLATOR
AMPLIFIER
POWER SUPPLY
A C VOLTMETER
PHOTOMULTIPLIER
VELOCITY MONITOR
DRIVER
D C VOLTMETER
A C VOLTMETER
PHASE METER
DUAL TRACE OSCILLOSCOPE
WAVE ANALYZER

a Phazor Model 210AB phase meter.

The drive head and cell assembly are shown in Figure 3. A black glass plane, one inch wide, was mounted at the lower end of the drive shaft. The drive shaft was held by four steel wires which confined the shaft to linear motion. The brass cell mounted below the driving head contained the solution to be investigated. The two opposite windows allowed the laser beam to pass through the solution, parallel to the plane. A thermistor was inserted through the side of the cell to monitor the temperature which was controlled by liquid passed through canals in the bottom of the brass cell.

To reveal the mechanical properties of polyethylene oxide, it was desired to find the relationship between the complex solution viscosity and the frequency of the shearing plane, using the described shear wave apparatus. This was accomplished by using the derived expression relating the measurable quantities α and β with the magnitude and phase of the viscosity (31). If α is the attenuation constant and β is $2\pi/$ shear wave length, then

$$|\eta| = \rho\omega/(\alpha^2+\beta^2) \qquad \text{(III-1)}$$

and

$$\phi = \tan^{-1}\left[\tfrac{1}{2}(\beta/\alpha - \alpha/\beta)\right] \qquad \text{(III-2)}$$

where

$$\eta^* = \eta' - i\eta'' = |\eta| e^{i\phi}. \qquad \text{(III-3)}$$

Figure 3. Diagram of Drive Head and Cell Assembly for Shear Wave Propagation System Showing Drive Coil A, Velocity Monitor B, Steel Wires of the Suspension System C, Glass Plane D, Reflector E, Fluid Cell F, System Supports G, Sliding Base H, and Thermistor I.

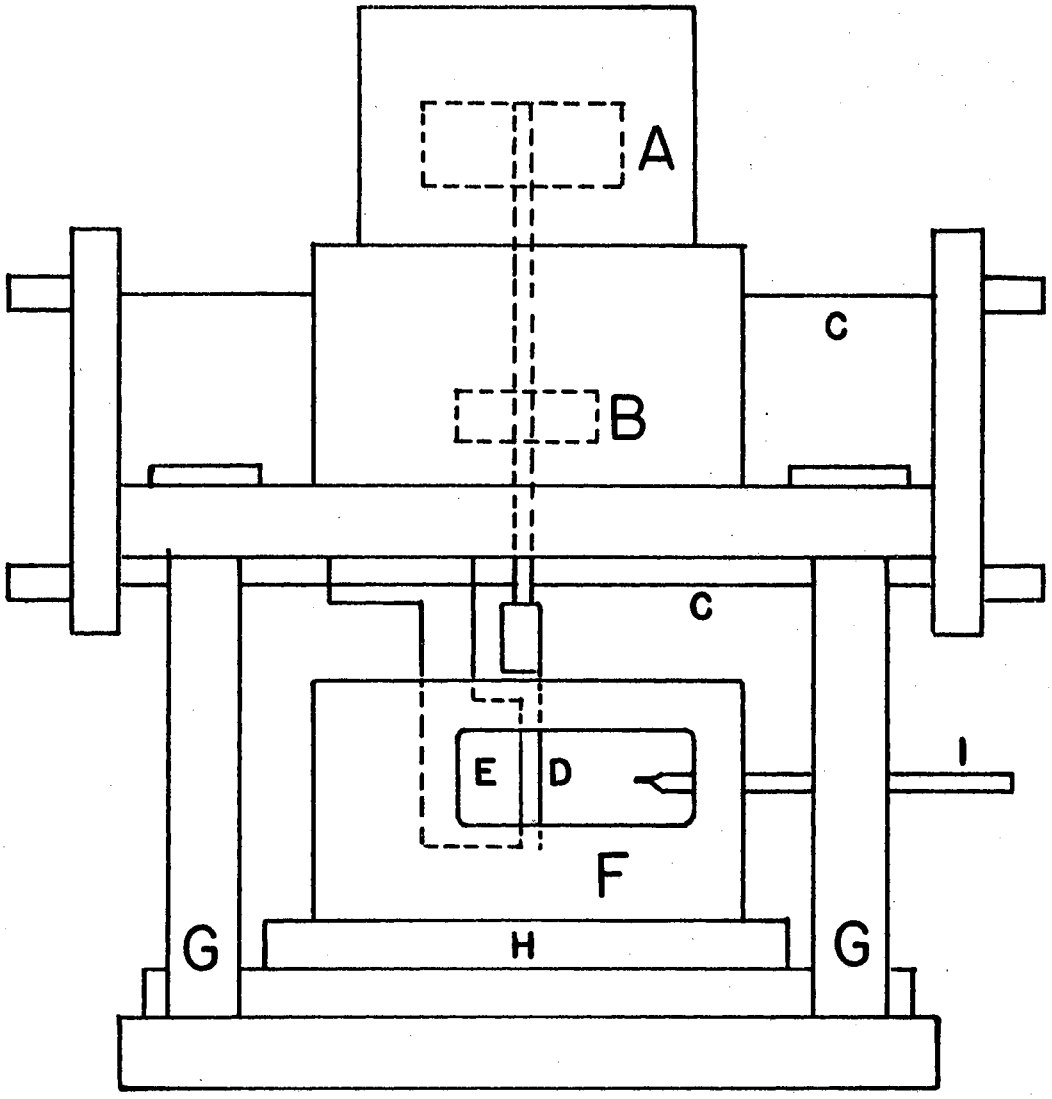
A
B
C
C
E
D
F
I
G
H
G

Since these expressions apply to shear waves originating from an infinite plane and to an infinite propagation field, the measurement conditions were limited to approximate these conditions. Using a one-inch plane, it was necessary to limit the shear wave length to 0.5 cm. If the shear wave length exceeded 1.0 cm, the effects of reflections were observed in fluctuations in the attenuation rate.

It was first necessary to determine the temperatures and frequencies to be investigated. As the viscosity of these aqueous solutions followed the same viscosity curve as did the solvent alone, 25°C was arbitrarily chosen for all measurements. As the viscosity of water can only be changed by a factor of 6 by temperature variation, the measurements at different temperatures would be of little help in reducing the relaxation curves to obtain greater frequency range. For this apparatus the lowest usable frequency was 15 cps. At frequencies below this the wave form became distorted. The upper frequency was limited by the optical sensitivity, the attenuation rate, and the wave length of the shear wave. For low viscosity solutions this frequency was 300 cps, while for the higher molecular weights and concentrations a frequency of 750 cps was possible. Next, the beam shifter was set so that the laser beam passed as close to the shear plane as possible, but far enough away so that no diffracted light would interfere with the measurement. Suitable distance increments were selected for magnitude and phase measurements in the propagation field so that the α and β curves could be determined. Ten or fifteen such data points were usually sufficient. This was done for each of the nine or ten frequencies used within the allowed range.

C. Steady Flow Viscosity Measurements

The Couette apparatus, as diagrammed in Figure 4 and 5, was used to obtain steady flow viscosity measurements. The fluid under investigation is placed between two concentric brass cylinders C1 and C2. The inner cylinder has a diameter of 2.000 inches, and the outer one, which rotates, has an inside diameter of 2.060 inches. Thus the width of the gap between the two cylinders through which the fluid is sheared measures .030 inches. The inner cylinder, 5 cm in length, is supported by a copper fiber F attached to bellows B which is supported by a mounting frame. The inner cylinder, or bob, is positioned by an air bearing A which allows for almost frictionless rotation of the bob assembly. The rotation of the bob is detected by the capacitor C. The capacitor is calibrated by a micrometer MC located on the frame. The outer cylinder is rotated by a pulley system P and a variable speed motor M.

In order to determine the zero shear rate viscosity, the relationship between the stress and the gradient must first be determined. The velocity gradient G in the center of the gap is given by (32)

$$G \simeq \frac{R_i + D/2}{D} \Omega \qquad \text{(III-4)}$$

where R_i is the radius of the inner cylinder, D is the gap width, and Ω is the angular velocity of the outer cylinder. This approximation holds for systems where $D \ll R_i$. For this system where R_i = 1.030" and D = 0.030", the gradient varies about 6 per cent across the gap. Using these values to calculate the gradient, the value of G at the center of the gap is less than one per cent

Figure 4. Diagram of the Couette System for the Measurement of Steady Flow Viscosity Showing Bellows B, Torsion Fiber F, Capacitor Plates C, Air Bearing A, and Concentric Cylinders C1 and C2.

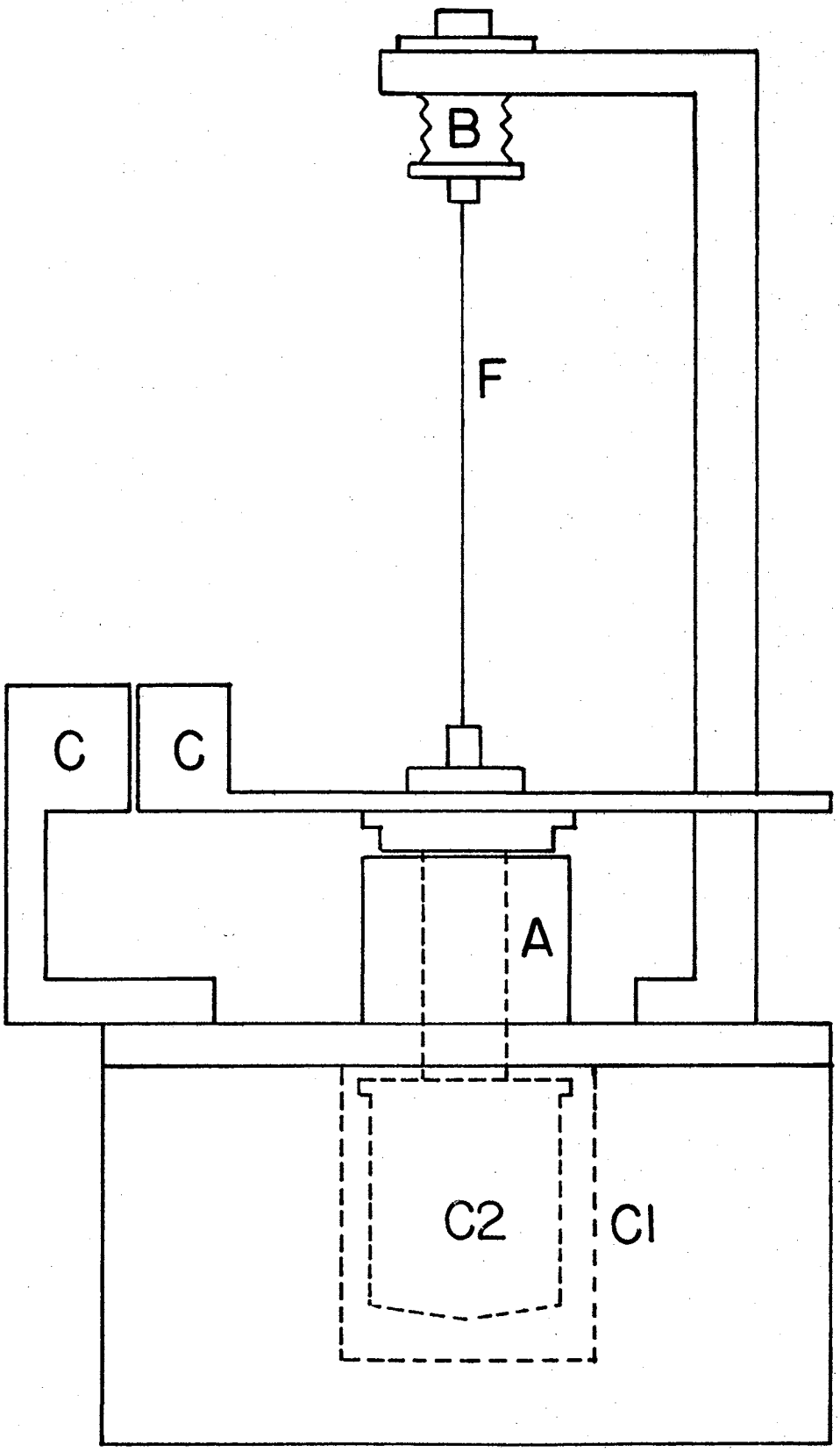
B
F
C
C
A
C2
C1

Figure 5. Diagram Illustrating the Top View of Couette System Showing Micrometer MC, Fiber Mounting F, Capacitor Plates C, Pulley System P, and Motor Pulley M.

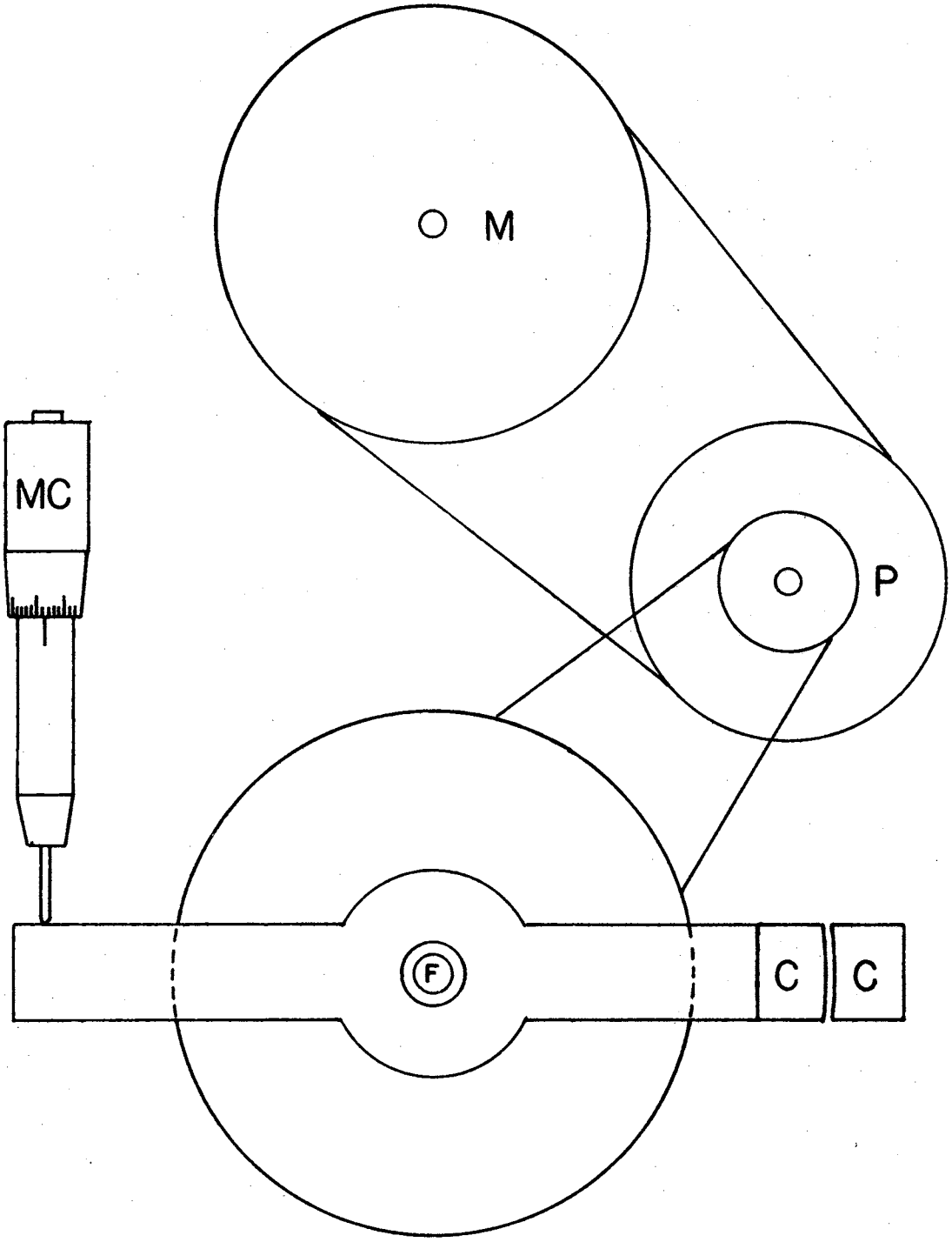
M
MC
P
F
C
C

different from the exact value.

A 1/15 horsepower Bodine motor with a variable speed control was used to rotate the outer cylinder. Velocity gradients from 1 to 644 per second could be obtained using this belt and pulley system. The gradient was measured by a counter, triggered by the output signal of a photodetector, which is located on one side of a slotted ring attached to the outer cylinder. The detector is activated when light passes through one of the twenty slots in the chopping ring. Substituting the proper dimensions into equation (III-4), the velocity gradient is given by

$$G = \frac{10.629}{T} \ sec^{-1} \qquad \text{(III-5)}$$

where T is the time interval measured in seconds.

The shearing stress is determined by measuring the torque exerted by the sheared fluid on the bob. For small angles the torque exerted on the bob is proportional to the angular displacement of the fiber. This displacement is detected by a change in capacitance when the capacitor plate attached to the bob is moved with respect to the stationary plate. This change in electrical capacitance is detected by a linear change in the frequency of a relaxation oscillator which includes the capacitor in the circuit.

A constant k_τ for this system is defined by

$$\Delta f \, k_\tau = \tau \qquad \text{(III-6)}$$

where Δf is the change in oscillator frequency with units of cps and τ is the torque on the fiber. k_τ has units of dyne-cm-sec. The steady flow viscosity is defined as

$$\eta = \text{stress}/G. \tag{III-7}$$

The stress is related to the torque by

$$\text{stress} = \frac{\tau}{2\pi R^2 \ell} \tag{III-8}$$

where R is the radius of the bob and ℓ is the length of the bob. Then, substituting equation (III-7) into (III-8) and (III-8) into (III-6),

$$k_\tau = \frac{\tau}{\Delta f} = \frac{\eta (2\pi R^2 \ell) G}{\Delta f}. \tag{III-9}$$

If Q is a bob constant with units of cm^3, such that and $Q = 2\pi R^2 \ell$, then

$$k_{\tau Q} = \frac{\eta G}{\Delta f}. \tag{III-10}$$

Since several different fibers are used, a fiber constant C_f is defined for each by

$$\tau = C_f \Delta\theta = C_f \frac{\Delta S}{r} \tag{III-11}$$

where ΔS is the change in arc length at radius r.

The measurement constant k_θ, relating angular displacement to oscillator frequency change, is defined by

$$k_\theta = \frac{\Delta\theta}{\Delta f} = \frac{\Delta S}{r} \cdot \frac{1}{\Delta f}. \tag{III-12}$$

Rearranging terms,

$$\Delta f k_\theta = \frac{\Delta S}{r} . \qquad \text{(III-13)}$$

Substituting equation (III-12) into (III-11),

$$\tau = c_f \Delta f k_\theta . \qquad \text{(III-14)}$$

Since the stress is related to the torque by a multiplying constant $1/Q$, and substituting equation (III-14) into (III-9), then,

$$k_{TQ} = c_{fQ} k_\theta \qquad \text{(III-15)}$$

where $c_{fQ} = c_f / Q$. Then from equation (III-7) the viscosity is related by

$$\eta = \frac{k_\theta c_{fQ} \Delta f}{G} . \qquad \text{(III-18)}$$

The value of k_θ is determined for each viscosity measurement by plotting the oscillator frequency against the micrometer setting. The resulting slope is then substituted into equation (III-16). The fiber constant c_{fQ} is determined by the measurement of fluids which have well defined viscosities. For this purpose water was used for the smaller fibers and glycerol for the larger fibers. For beryllium copper fibers the values of c_{fQ} ranged from 8.85×10^2 dynes/cm^2 to 7.30×10^4 dynes/cm^2 for fibers of diameters 0.0417 to 0.125 inches.

Couette viscosity data are obtained by the measurement of stress on the bob at different gradients. After the sample under investigation is brought to a constant temperature by passing a controlling

fluid through passages in the outer cylinder, the bob assembly shown in Figures 4 and 5 is adjusted for proper sensitivity. This is done by setting the capacitator plates such that the value of K_ϕ is constant over the greatest possible displacement. If the quiescent frequency is 110 kilocycles, a linear range of 6 kilocycles can be obtained. This is approximately 2.5 mm of arc as measured by the micrometer. The change in oscillator frequency and the corresponding gradients are recorded. Using equation (III-16) the viscosity for each gradient can be calculated. To find viscosities over the complete gradient range it was often necessary to use more than one size fiber.

CHAPTER IV

EXPERIMENTAL RESULTS

A. Steady Flow Viscosity

In order to reduce the oscillatory shear data, it was first necessary to determine the viscosity corresponding to shear rates approaching zero. For solutions displaying Newtonian characteristics, only a few low velocity gradient measurements were needed to make this determination, since for a Newtonian material the viscosity is not a function of the gradient. The steady flow viscosity of polyethylene oxide solutions was not constant, even at low gradients. In Figure 6 this is demonstrated for polyethylene oxide WSR-301, which has a molecular weight of approximately 4,000,000. Here the stress is plotted against the product of the gradient and the extrapolated zero shear rate viscosity for four concentrations. The extrapolation is accomplished by plotting the stress versus the gradient on log-log paper, determining for the resulting curve the point where the ratio of stress to gradient becomes constant, as represented by a 45° line which the data curve would apparently join if lower gradient data were available. Below the juncture of the curve and the line the viscosity is independent of gradient, and hence equals the zero shear rate viscosity.

The dashed line represents the behavior of a Newtonian fluid. The point at which the data curve breaks away from the dashed line is

Figure 6. Stress τ Versus the Product of Velocity Gradient G and Extrapolated Steady Flow Viscosity η_o for Four Concentrations of Polyethylene Oxide of Molecular Weight 4×10^6.

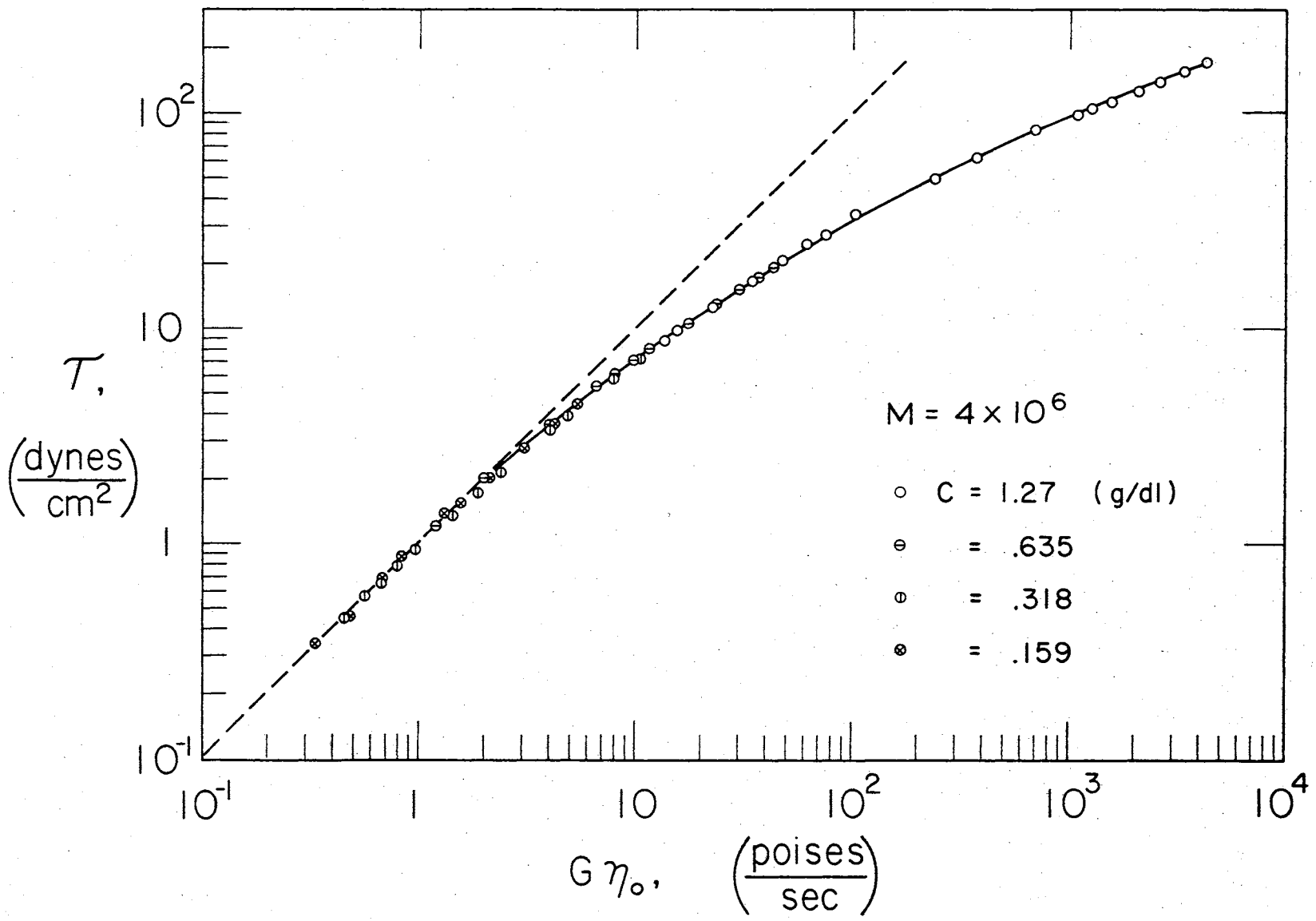
10^2
10
1
10^{-1}
τ, $\left(\frac{\text{dynes}}{\text{cm}^2}\right)$
10^{-1}
1
10
10^2
10^3
10^4
$G\eta_o$, $\left(\frac{\text{poises}}{\text{sec}}\right)$
M = 4×10^6
○ C = 1.27 (g/dl)
⊖ = .635
⊖ = .318
⊗ = .159

independent of concentration but is dependent on molecular weight. From the data obtained for lower molecular weights the "breakaway" point occurred at higher stress values. It is concluded that the extent of Newtonian character of this material is dependent on molecular weight. Since high molecular weights of polyethylene oxide in solutions of sufficient concentration such that the viscoelastic properties differ measurably from that of the solvent do not have a Newtonian character, it is concluded that there is extensive interaction and perhaps some permanent deformation of the molecule when subjected to high gradients.

The specific viscosity is defined as

$$\eta_{sp} = \frac{\eta_o - \eta_s}{\eta_s} \qquad \text{(IV-1)}$$

where η_s is the solvent viscosity and η_o is the zero shear rate viscosity. The intrinsic viscosity is defined as

$$[\eta]_o = \lim_{\substack{c \to 0 \\ q \to 0}} \frac{\eta_o - \eta_s}{\eta_s c} \qquad \text{(IV-2)}$$

where c is the concentration. If the concentration is given in gm/dl the intrinsic viscosity will have units of dl/gm. A new quantity k is defined by the relation

$$k[\eta]_o = \frac{\eta_o - \eta_s}{\eta_s c_k} \qquad \text{(IV-3)}$$

where c_k is the concentration of the solution characterized by the quantity k. For each concentration there is a particular value by which the intrinsic viscosity is multiplied to give the specific viscosity.

The values of k for five polymer samples can be determined

from Figure 7. The polymers of molecular weights .064 x 10^6, .170 x 10^6, and .480 x 10^6 were laboratory samples furnished by Union Carbide Corporation; that of 1.1 x 10^6 was obtained from the Centre de Recherches sur les Macromolecules, Strasbourg, France, and that of 4 x 10^6 was a commercial grade manufactured by Union Carbide. In Figure 7 the specific viscosity divided by the concentration is plotted against the concentration. Each dashed line indicates the limiting value of η_{sp}/C, which is the intrinsic viscosity for that molecular weight. For any concentration the value of k can be determined by dividing the value of η_{sp}/C_K by the limiting value η_{sp}/C_{CRIT}. The point at which the curve joins the horizontal line, the intrinsic value, is called the critical concentration C_{crit}. For concentrations less than this the value of η_{sp}/C is equal to $[\eta]_o$, and thus $k = 1$.

It was often useful to prepare solutions of different molecular weights but with a constant k value. The desired concentration could be determined from Figure 8. Here the polymer concentration is plotted against the molecular weight for selected values of k. These curves may be thought of as "curves of constant interaction."

The intrinsic viscosity is related to the molecular weight by

$$[\eta]_o = a M^P \qquad \text{(IV-4)}$$

where a is a multiplying constant with the proper units and P is a constant with a value between .5 and 1.0. The values of a and P can be obtained from Figure 9, where the intrinsic viscosity is plotted against the molecular weight. For aqueous solutions of polyethylene oxide at 25°C,

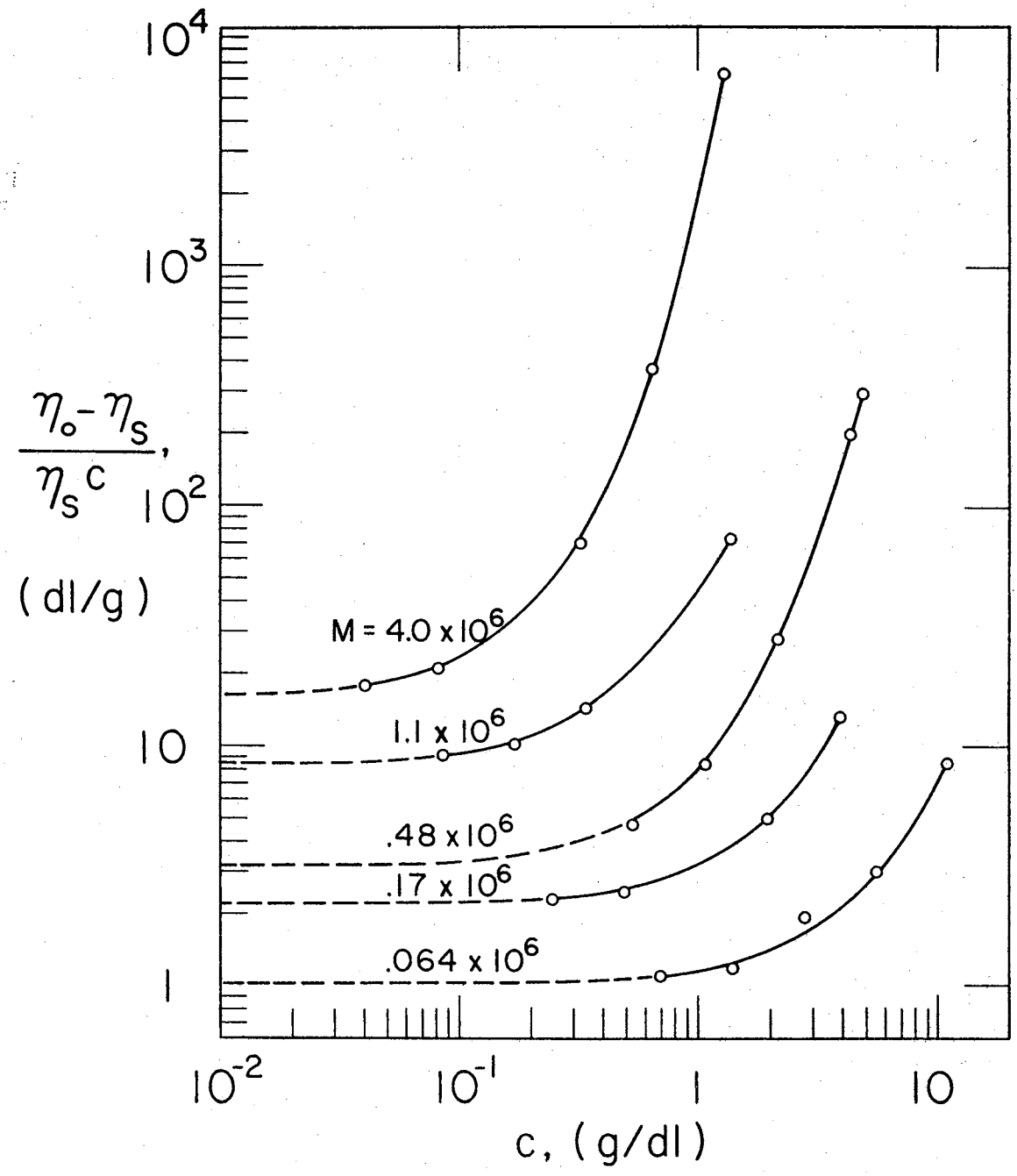
10^4
10^3
10^2
10
1
$\frac{\eta_o - \eta_s}{\eta_s c}$,
(dl/g)
M = 4.0 x 10^6
1.1 x 10^6
.48 x 10^6
.17 x 10^6
.064 x 10^6
10^{-2}
10^{-1}
1
10
c, (g/dl)

Figure 8. Concentration c Versus Molecular Weight M for Selected Values of k for Aqueous Solutions of Polyethylene Oxide. T = 25°C.

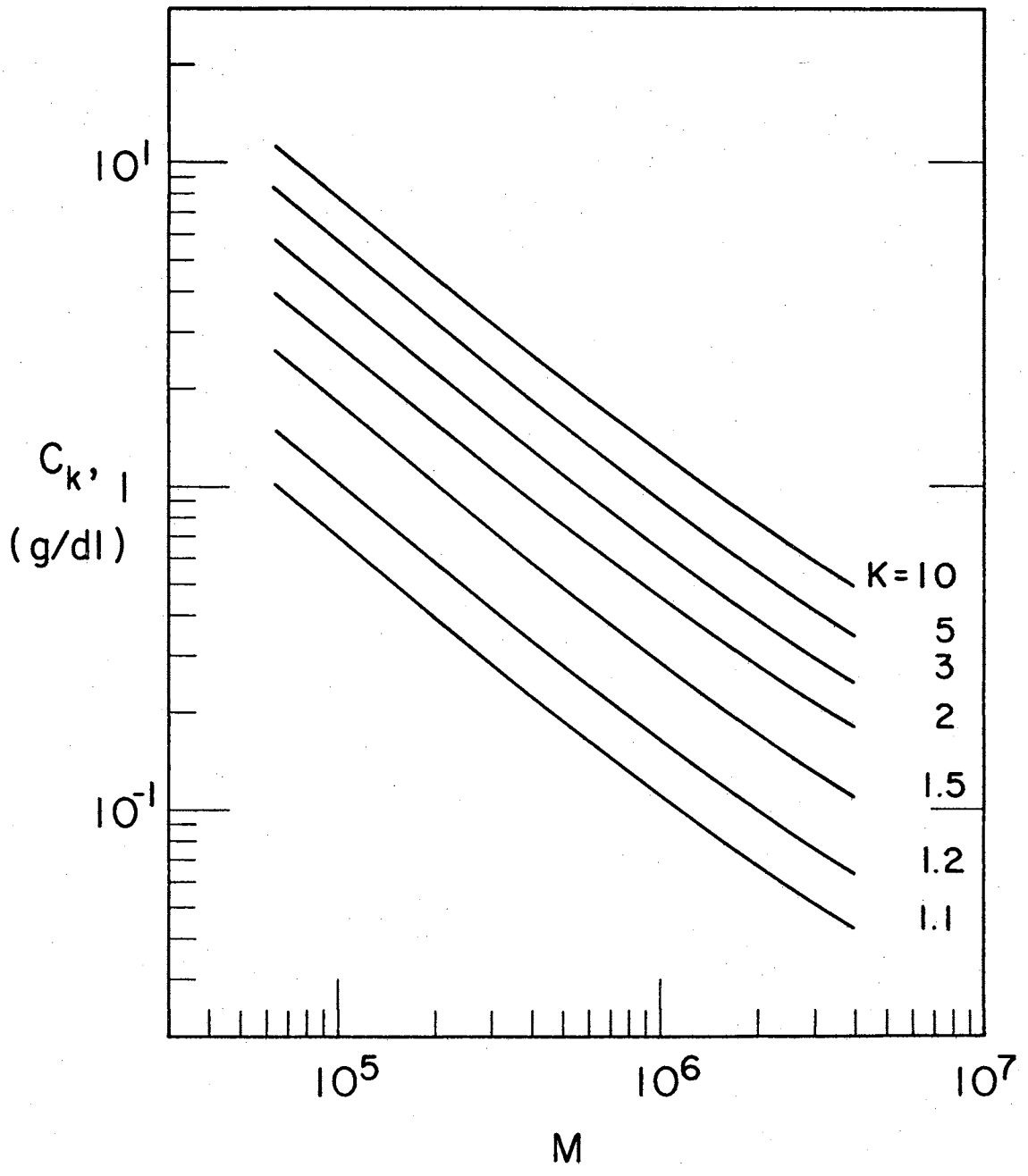
10^1
C_k, l
(g/dl)
10^{-1}
K=10
5
3
2
1.5
1.2
1.1
10^5
10^6
10^7
M

Figure 9. Extrapolated Intrinsic Viscosities $[\eta]_o$ Versus Molecular Weight for Aqueous Solutions of Polyethylene Oxide. T = 25°C.

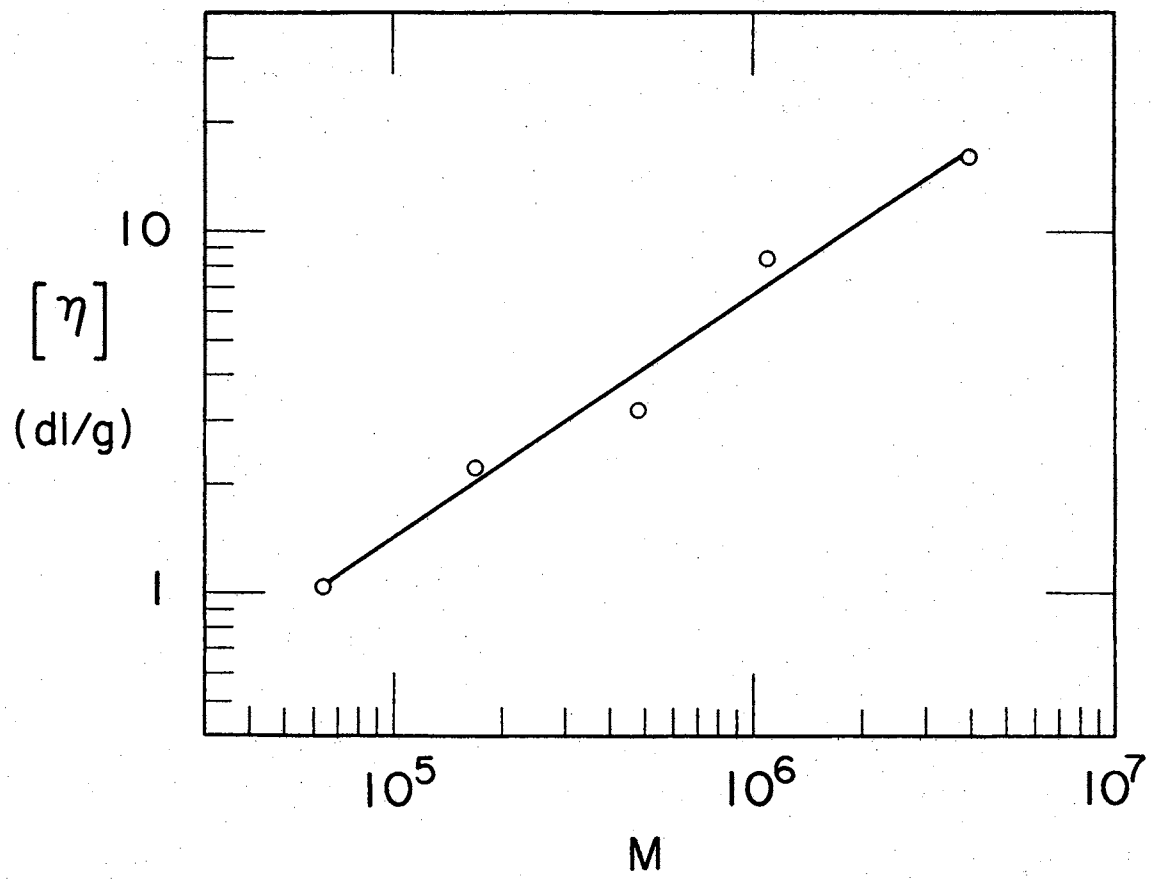
10
[η]
(dl/g)
1
10^5
10^6
10^7
M

$$[\eta]_o = 1.0 \times 10^{-4} M^{0.83} \text{ dl/g} \quad . \tag{IV-5}$$

This agrees well with values previously determined (6, 33). The discrepancies in the values of a and P may be due to differences in solution preparation procedures or methods of extrapolation.

B. Shear Wave Propagation Results

Using the procedures outlined in Chapter III, the viscoelastic properties of the solutions represented by η and ϕ_η were determined for many samples. Since it was desired to investigate the complex viscosity of the polymer as a function of frequency, it was necessary to correct for the solvent viscosity. This was easily accomplished by subtracting the solvent viscosity η_s from the real part of the solution viscosity. Then

$$|\eta^* - \eta_s|^2 = (\eta' - \eta_s)^2 + (\eta'')^2 \tag{IV-6}$$

and

$$|\eta^* - \eta_s| = \left[(\eta' - \eta_s)^2 + (\eta'')^2 \right]^{1/2} \tag{IV-7}$$

Substituting with trigonometric functions, equation (IV-7) becomes

$$|\eta^* - \eta_s| = \left[(\eta \cos\phi_\eta - \eta_s)^2 + \eta^2 \sin^2 \phi_\eta \right]^{1/2} \tag{IV-8}$$

where $\eta \cos\phi_\eta = \eta'$ and $\eta \sin\phi_\eta = \eta''$, and the corrected phase angle is

$$\tan\psi = \frac{\eta''}{\eta' - \eta_s} = \frac{\eta \sin\phi_\eta}{\eta\cos\phi_\eta - \eta_s} \quad . \tag{IV-9}$$

Four solutions of different molecular weight were prepared such that the value of k was 10. This was accomplished by adjusting the concentration according to Figure 8. It was found that when was less than 10, the properties of the solution did not differ significantly from those of pure water, thus making measurements difficult. In Figure 10 the corrected magnitude and phase are plotted as functions of frequency. The value of the magnitude is normalized by dividing the complex viscosity magnitude by $\eta_0-\eta_s$, where η_0 is the zero shear viscosity obtained from steady flow viscosity measurements. For low frequencies the magnitude of the oscillatory shear viscosity approaches the value of $\eta_0-\eta_s$. From this figure, it can be seen that for a particular frequency the value of the phase and magnitude depends on molecular weight.

The variation of the other parameter, k , is reflected in Figure 11. With a constant molecular weight, 480,000, four solutions of different k values were measured. Plotted in the same manner as in Figure 10, the magnitude and phase showed a similar dependence on k for a particular frequency.

Figure 12 shows the relationship among solutions of the same molecular weight at three different levels of k . Here, polyethylene oxide WSR-301 was used to prepare solutions where k equaled 2, 10, and 100. In this case, the value of the phase angle remains constant over the frequency range for all values of k . Not even for the lowest value of k does the normalized value of the magnitude approach 1 horizontally. These results reflect the same character observed for steady flow measurements.

Figure 10. Magnitude $|\eta^* - \eta_s| / (\eta_o - \eta_s)$ and Phase ψ Versus Frequency for Aqueous Solutions of Polyethylene Oxide of Differing Molecular Weights Having a Constant Value of K Equal to 10. T = 25°C.

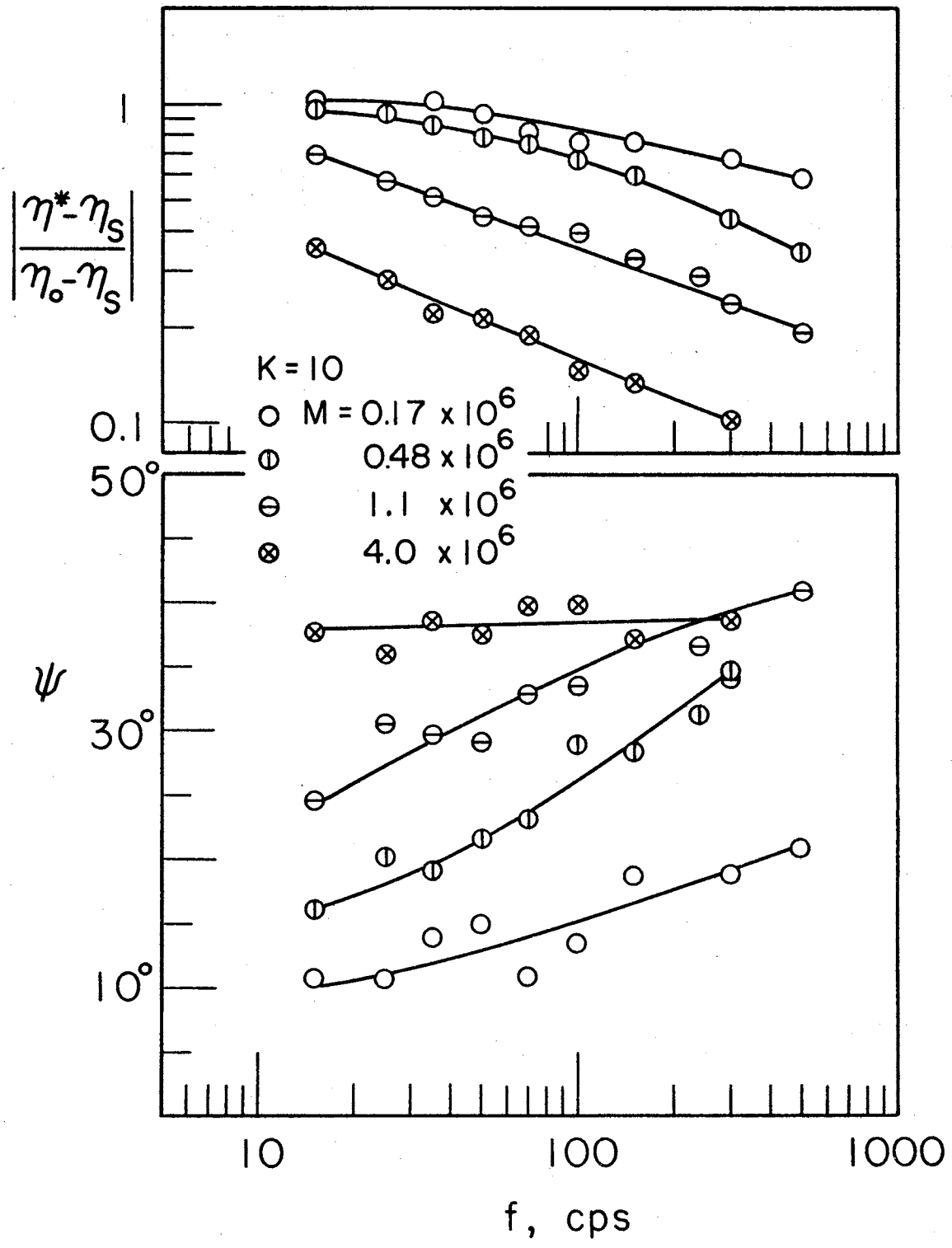
1
0.1
$\left|\frac{\eta^*-\eta_s}{\eta_o-\eta_s}\right|$
K = 10
M = 0.17 x 10^6
0.48 x 10^6
1.1 x 10^6
4.0 x 10^6
50°
30°
10°
ψ
10
100
1000
f, cps

Figure 11. Magnitude $|\eta^* - \eta_s| / (\eta_o - \eta_s)$ and Phase Angle ψ Versus Frequency for Aqueous Solutions of Polyethylene Oxide of Molecular Weight 480,000. T = 25°C.

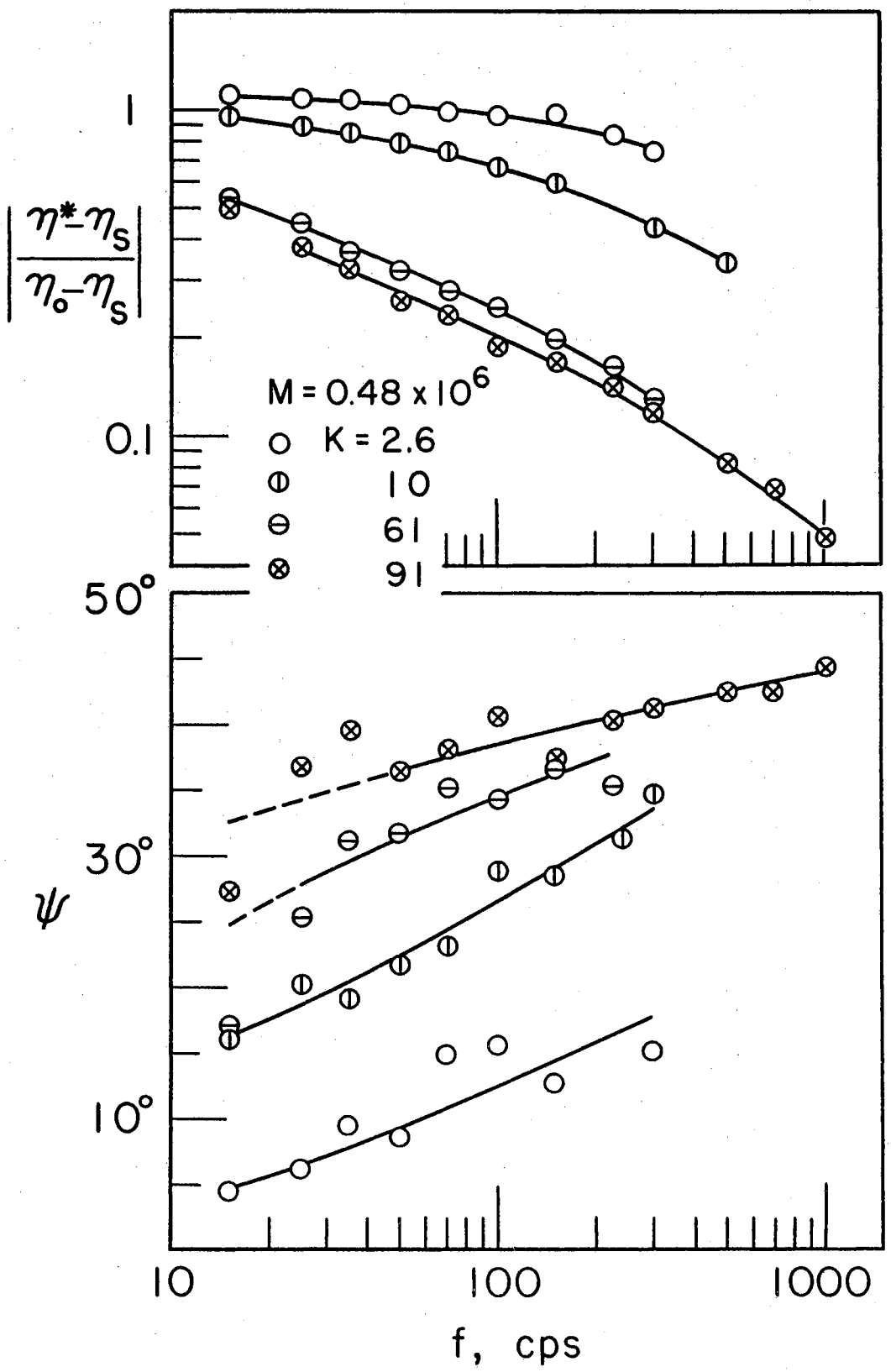
1
0.1
$\left|\frac{\eta^*-\eta_s}{\eta_o-\eta_s}\right|$
M = 0.48 x 10^6
K = 2.6
10
61
91
50°
30°
10°
ψ
10
100
1000
f, cps

Figure 12. Magnitude $|\eta^* - \eta_s| / (\eta_o - \eta_s)$ and Phase Angle ψ Versus Frequency for Aqueous Solutions of Polyethylene Oxide of Molecular Weight 4×10^6. T = 25°C.

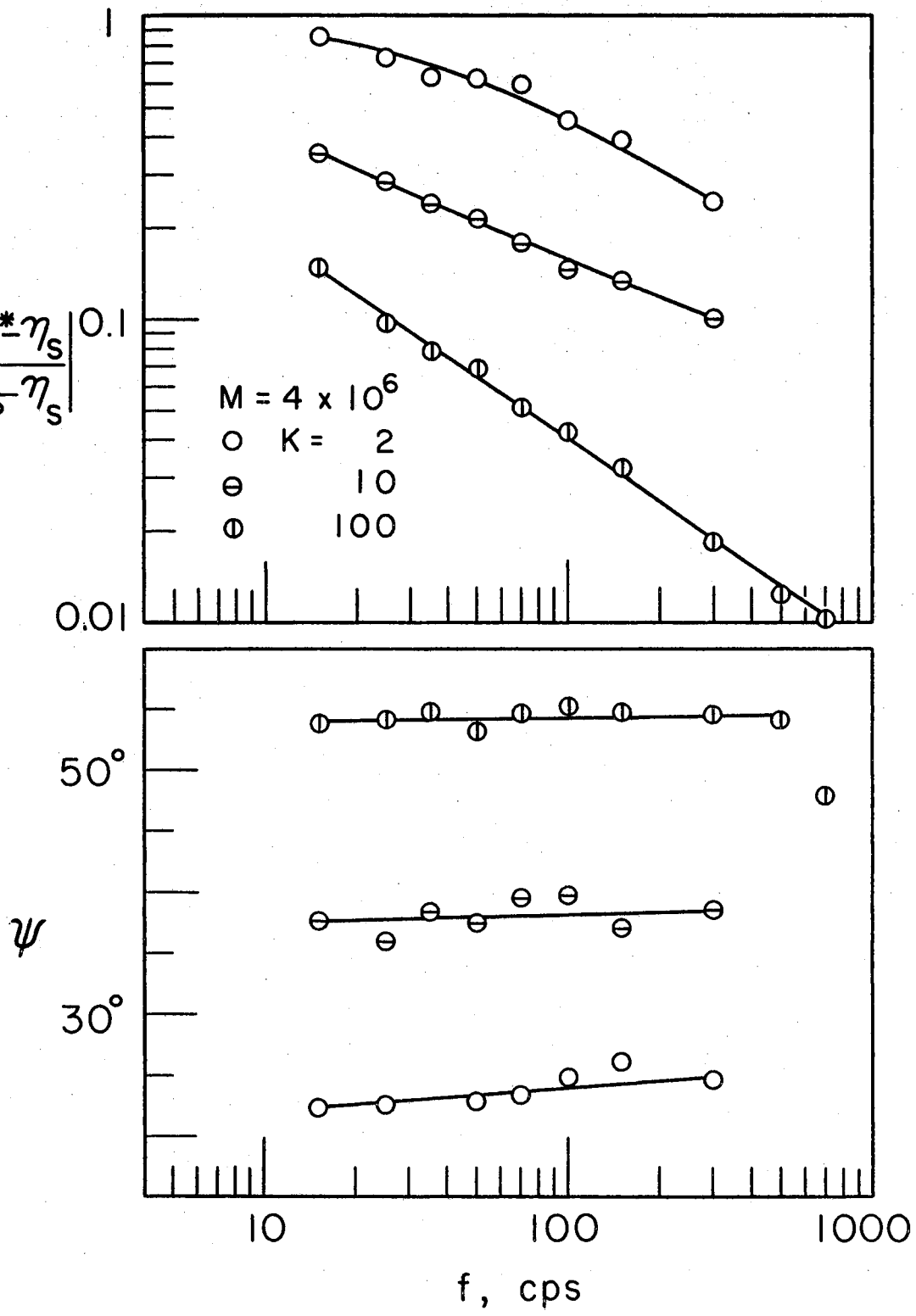
1
0.1
0.01
$\left|\frac{\eta^*-\eta_s}{\eta_o-\eta_s}\right|$
M = 4 x 10^6
K = 2
10
100
50°
30°
ψ
10
100
1000
f, cps

CHAPTER V

DISCUSSION OF RESULTS

A. Comparison with the Zimm Theory

In comparing the results to the Zimm theory for dilute solutions, the extension developed in Chapter II is employed. For the two cases selected, (1) the variation of molecular weight at constant temperature and constant k and (2) the variation of k holding the temperature and molecular weight constant, the data was shifted using reduction functions a_M and a_c respectively, using arbitrary reference values. The reduced data was then superimposed on theoretical curves given by the Zimm theory. The positioning of the data was determined by the best fit to the theoretical curves. Since the theoretical curves determine the value of the phase and magnitude of the complex viscosity as a function of frequency times the longest relaxation time τ_1, the value of τ_1 can be determined for each set of data.

Figures 13 and 14 show the data given in Figure 10 reduced according to the a_M function defined by equation (II-56). The longest relaxation times τ_1 are given for each molecular weight, as determined from the theoretical curves. The solid lines are the theoretical relaxation curves for molecules having 2000, 100, and 10 segments for the non-free-draining condition (26). It should be noted that as the molecular weight increases, the number of segments also increases. This may partly explain the need for several theoretical curves to define

Figure 13. Magnitude $|\eta^* - \eta_s| / (\eta_o - \eta_s)$ Versus $\omega\tau_1$ for Aqueous Solutions of Polyethylene Oxide with the Value of k Equal to 10, Reduced by the a_M Function and Superimposed on the Zimm Relaxation Curves for a Non-free-draining Molecule. T = 25°C.

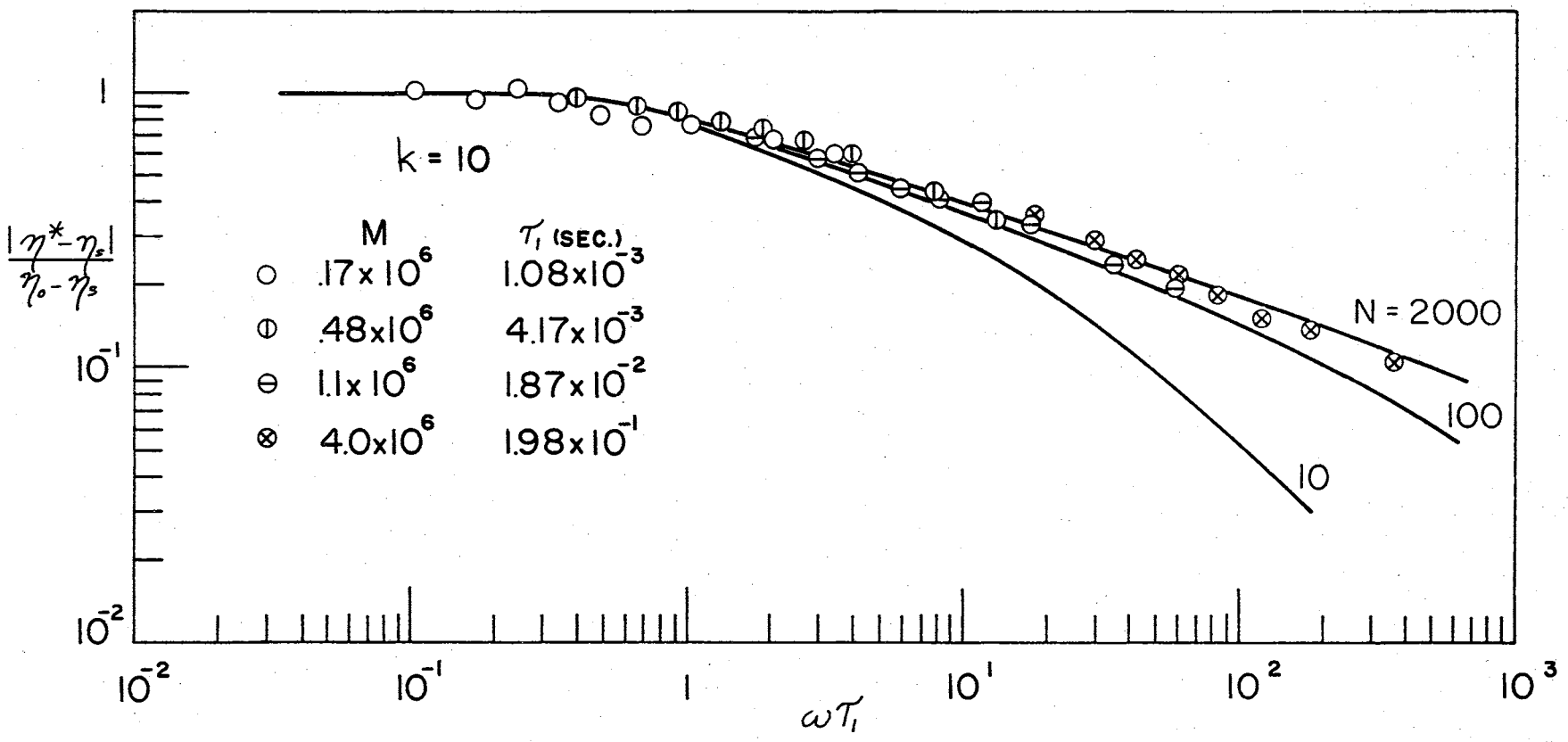
1
10^{-1}
10^{-2}
$\frac{|\eta^* - \eta_s|}{\eta_0 - \eta_s}$
k = 10
M
τ_1 (SEC.)
○ .17x10^6 1.08x10^-3
◐ .48x10^6 4.17x10^-3
⊖ 1.1x10^6 1.87x10^-2
⊗ 4.0x10^6 1.98x10^-1
N = 2000
100
10
10^{-2}
10^{-1}
1
10^{1}
10^{2}
10^{3}
$\omega\tau_1$

Figure 14. Phase Angle ψ Versus $\omega\tau_1$ for Aqueous Solutions of Polyethylene Oxide with the Value of k Equal to 10, Reduced by the a_M Function and Superimposed on the Zimm Relaxation Curves for a Non-free-draining Molecule. T = 25°C.

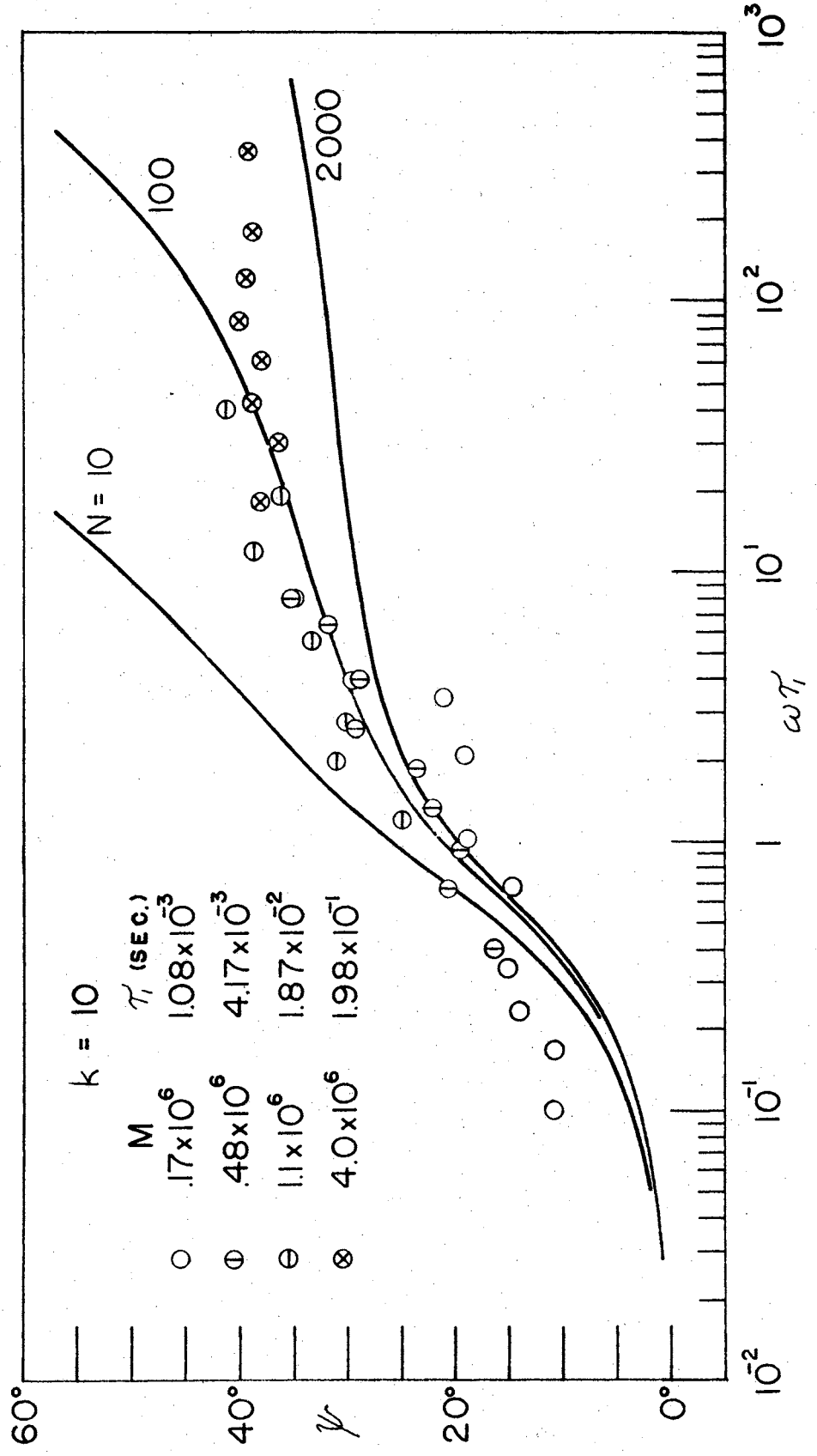
60°
40°
20°
0°
ψ
10^-2
10^-1
1
10^1
10^2
10^3
ωτ1
N = 10
100
2000
k = 10
M
τ1 (SEC.)
.17×10^6
1.08×10^-3
.48×10^6
4.17×10^-3
1.1×10^6
1.87×10^-2
4.0×10^6
1.98×10^-1

the reduced experimental curve. These relaxation times are plotted against molecular weight in Figure 15. In the same figure the theoretical values of τ_1 obtained from the relation

$$\tau_1 = \frac{[\eta]_0 M \eta_s C}{N_a k T} \qquad \text{(V-1)}$$

are shown where

$$C = 1 \Big/ \sum_{P=1}^{N} \lambda_1/\lambda_P \qquad \text{(V-2)}$$

and (27)

$$C \simeq .42 \qquad \text{(V-3)}$$

for non-free-draining chains. These theoretical values of τ_1 were computed using the results of the Zimm theory and the steady flow viscosity values extrapolated to low gradients. The experimental values of τ_1 were determined by superposition of oscillatory shear data on the theoretical Zimm curves. The large difference in the resulting τ_1 values may be due to concentration effects not accounted for in the extension of the Zimm theory. This does not seem likely since the τ_1 values do not appear to approach a single value as k is decreased. Another possibility in evidence from the data is that the solution forms some sort of structure which is not altered in oscillatory shear measurements but is broken down when subjected to steady flow.

Figures 16 and 17 show the data from Figure 11 reduced according to the a_c function for a molecular weight of 480,000. The τ_1's are calculated for each value of k, for k ranging from 2.6 to

Figure 15. The Longest Relaxation Time τ_1 Versus Molecular Weight M for Aqueous Solutions of Polyethylene Oxide Determined from Reduced Oscillatory Shear Measurements and Steady Flow Measurements of the Intrinsic Viscosity. T = 25°C.

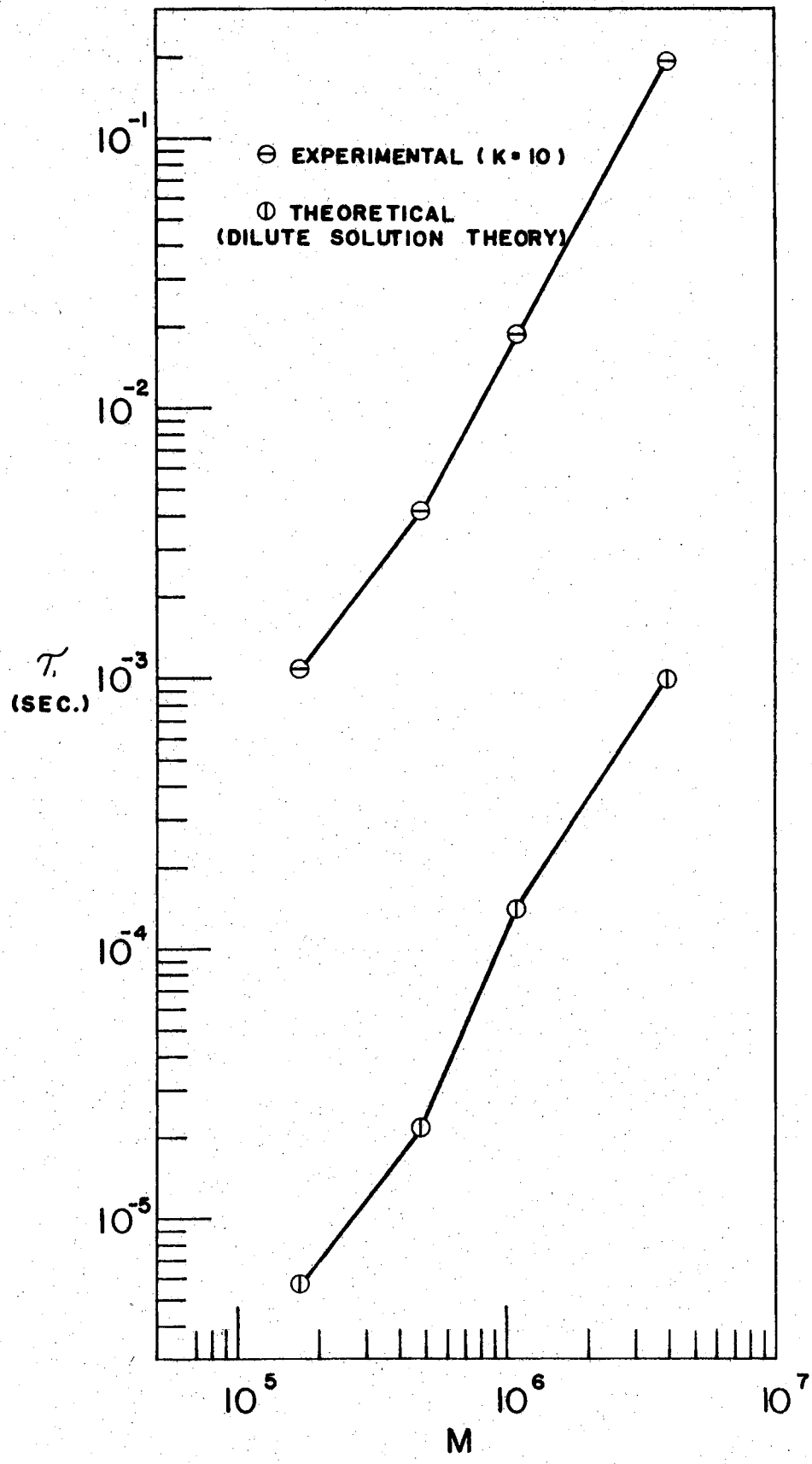
⊖ EXPERIMENTAL (K • 10)
◐ THEORETICAL
(DILUTE SOLUTION THEORY)
10^{-1}
10^{-2}
10^{-3}
10^{-4}
10^{-5}
τ
(SEC.)
10^{5}
10^{6}
10^{7}
M

Figure 16. Magnitude $|\eta^* - \eta_s| / (\eta_o - \eta_s)$ Versus $\omega\tau_1$ for Aqueous Solutions of Polyethylene Oxide with Molecular Weight of 480,000 Reduced by the a_c Function and Superimposed on the Zimm Relaxation Curves for a Non-free-draining Molecule. T = 25°C.

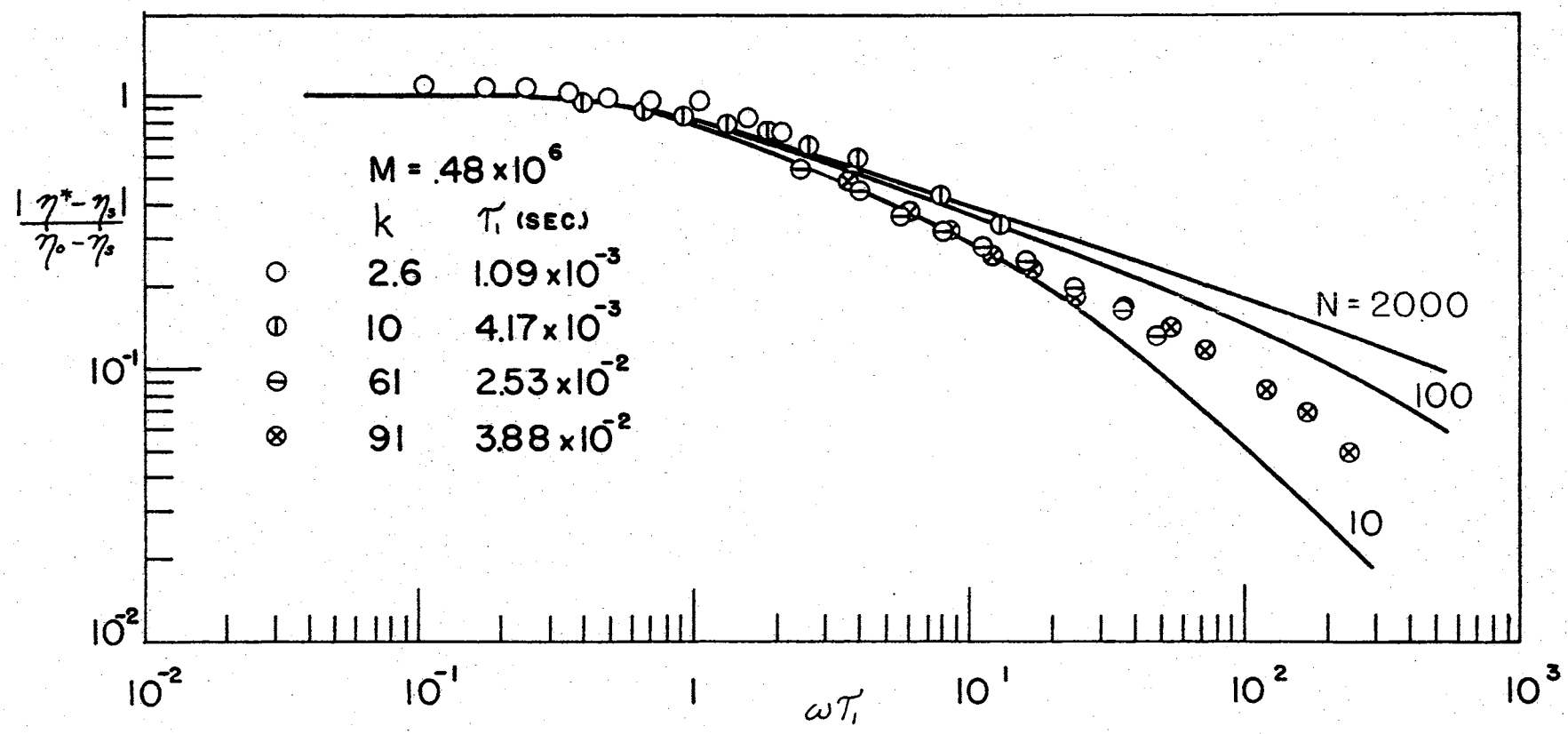
$\frac{|\eta^* - \eta_s|}{\eta_o - \eta_s}$
1
10^{-1}
10^{-2}
$M = .48 \times 10^6$
k
τ_1 (SEC.)
2.6 1.09×10^{-3}
10 4.17×10^{-3}
61 2.53×10^{-2}
91 3.88×10^{-2}
N = 2000
100
10
10^{-2}
10^{-1}
1
$\omega\tau_1$
10^1
10^2
10^3

Figure 17. Phase Angle Ψ Versus $\omega\tau_1$ for Aqueous Solutions of Polyethylene Oxide with Molecular Weight of 480,000 Reduced by the a_c Function and Superimposed on the Zimm Relaxation Curves for a Non-free-draining Molecule. T = 25°C.

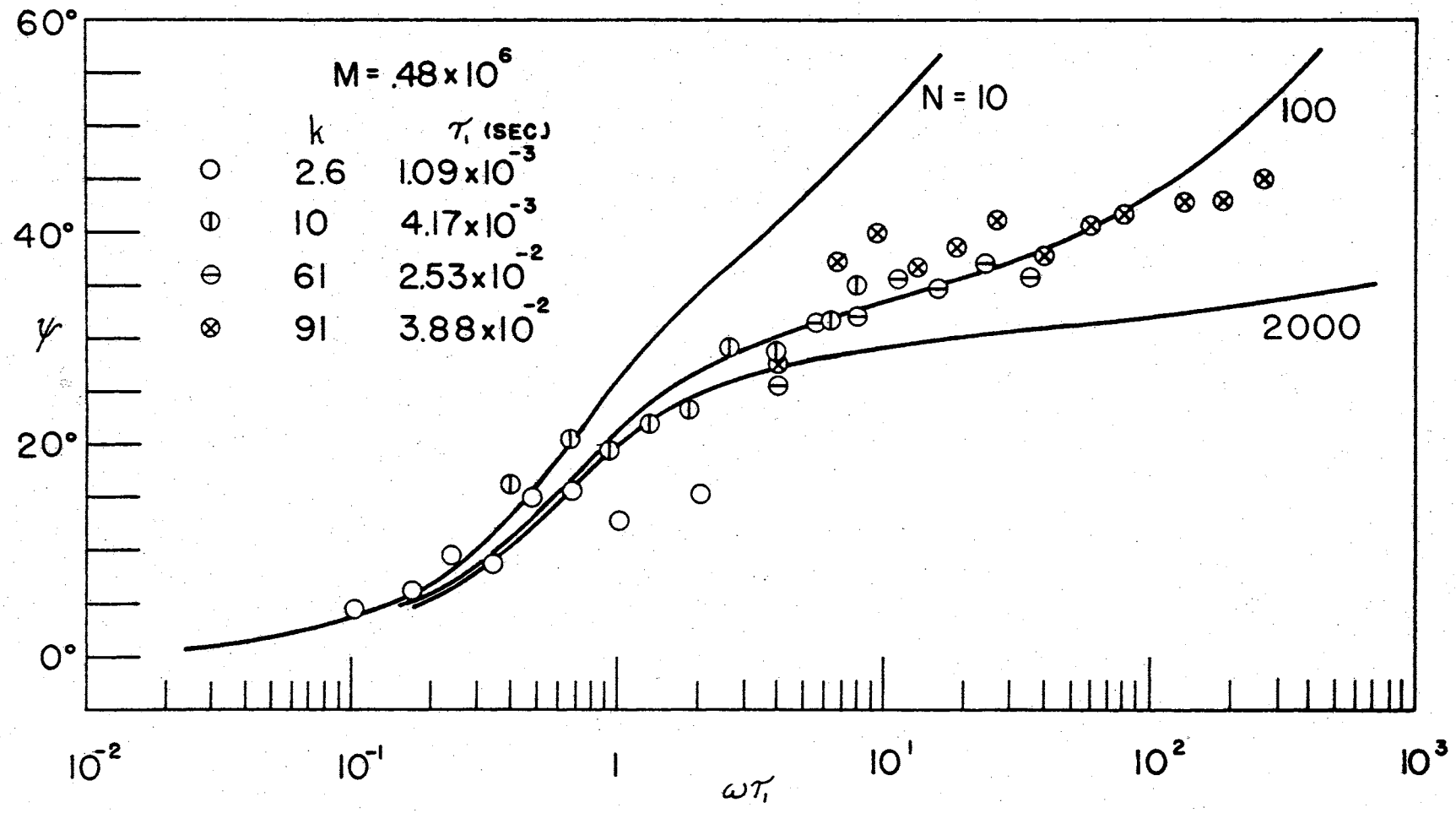
60°
40°
20°
0°
ψ
M = .48 x 10^6
k
τ1 (SEC)
2.6
1.09 x 10^-3
10
4.17 x 10^-3
61
2.53 x 10^-2
91
3.88 x 10^-2
N = 10
100
2000
10^-2
10^-1
1
10^1
10^2
10^3
ωτ1

91. As the data for this case did not appear to shift in the proper manner, the data was shifted according to an arbitrary best fit. Figures 18 and 19 show this shifted data superimposed on the theoretical relaxation curves. A different set of τ_1 values was determined according to this superposition.

The resulting τ_1 values from Figures 16, 17, 18, and 19 are plotted against the values of k in Figure 20. The τ_1's resulting from the data shifted according to the a_c function are linearly related to the value k. Thus the line joining the points has a 1st power slope on a log-log plot. The τ_1's resulting from the "best fit" shift are not linearly related to the values of k. The slope of a line approximating this case is 1.2 on a log-log plot. If this relation is approximated in such a way, then τ_1 is proportional to $k^{1.2}$ for this case.

When the a_c function was applied to the data shown in Figure 12, the reduction scheme failed. For a molecular weight of 4×10^6, the data obtained could not be shifted so as to superimpose the reduced curve on the theoretical relaxation curves with any reasonable success. It is apparent that the function was not applicable to such a high molecular weight solution at that concentration.

Considering these results, the reduction functions a_M and a_c give the approximate shifts for a good comparison with the theoretical model developed by Zimm.

Several effects which may be occurring in these solutions are not accounted for in the reduction functions. One of these is due to the addition of small quantities of Baymal to the polymer solutions. From data obtained for shear wave propagation measurements of .3 per cent

Figure 18. Magnitude $|\eta^* - \eta_s| / (\eta_o - \eta_s)$ Versus $\omega\tau_1$ for Aqueous Solutions of Polyethylene Oxide with Molecular Weight of 480,000 Shifted by Arbitrary Best Fit to the Zimm Relaxation Curves for a Non-free-draining Molecule. T = 25°C.

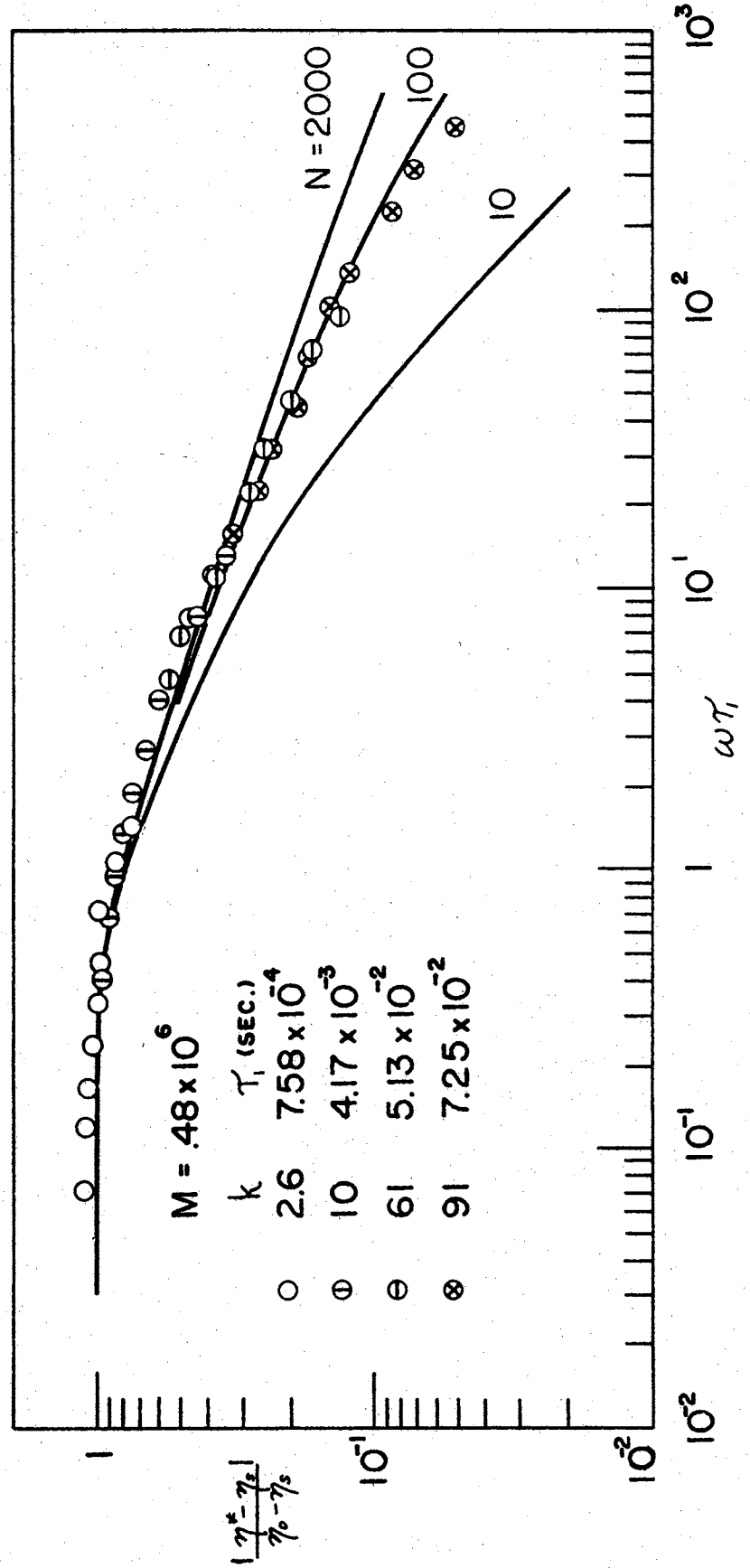
N = 2000
100
10
M = .48 x 10^6
k
τ1 (SEC.)
2.6
7.58 x 10^-4
10
4.17 x 10^-3
61
5.13 x 10^-2
91
7.25 x 10^-2
|η* - η'| / (η0 - η's)
ωτ1
1
10^-1
10^-2
10^-1
1
10^1
10^2
10^3

Figure 19. Phase Angle Ψ Versus $\omega\tau_1$ for Aqueous Solutions of Polyethylene Oxide with Molecular Weight of 480,000 Shifted by Arbitrary Best Fit to the Zimm Relaxation Curves for a Non-free-draining Molecule. T = 25°C.

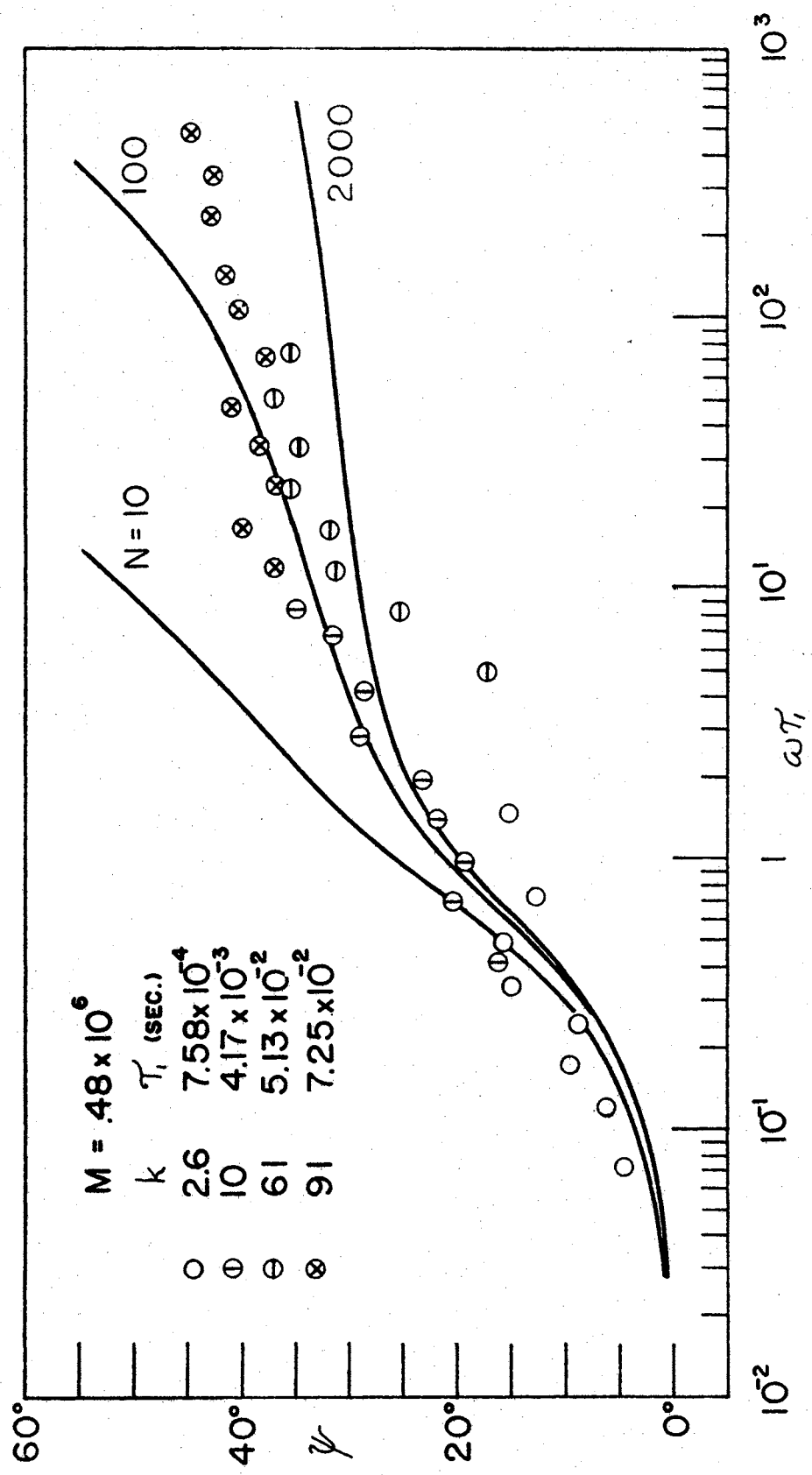
M = .48 x 10^6
k
τ1 (SEC.)
2.6
7.58x10^-4
10
4.17x10^-3
61
5.13x10^-2
91
7.25x10^-2
N = 10
100
2000
ψ
ωτ1
60°
40°
20°
0°
10^-2
10^-1
1
10^1
10^2
10^3

Figure 20. The Longest Relaxation Time τ_1 Versus k for Aqueous Solutions of Polyethylene Oxide with Molecular Weight of 480,000, Determined from Best Fit Data and a_c Reduction.

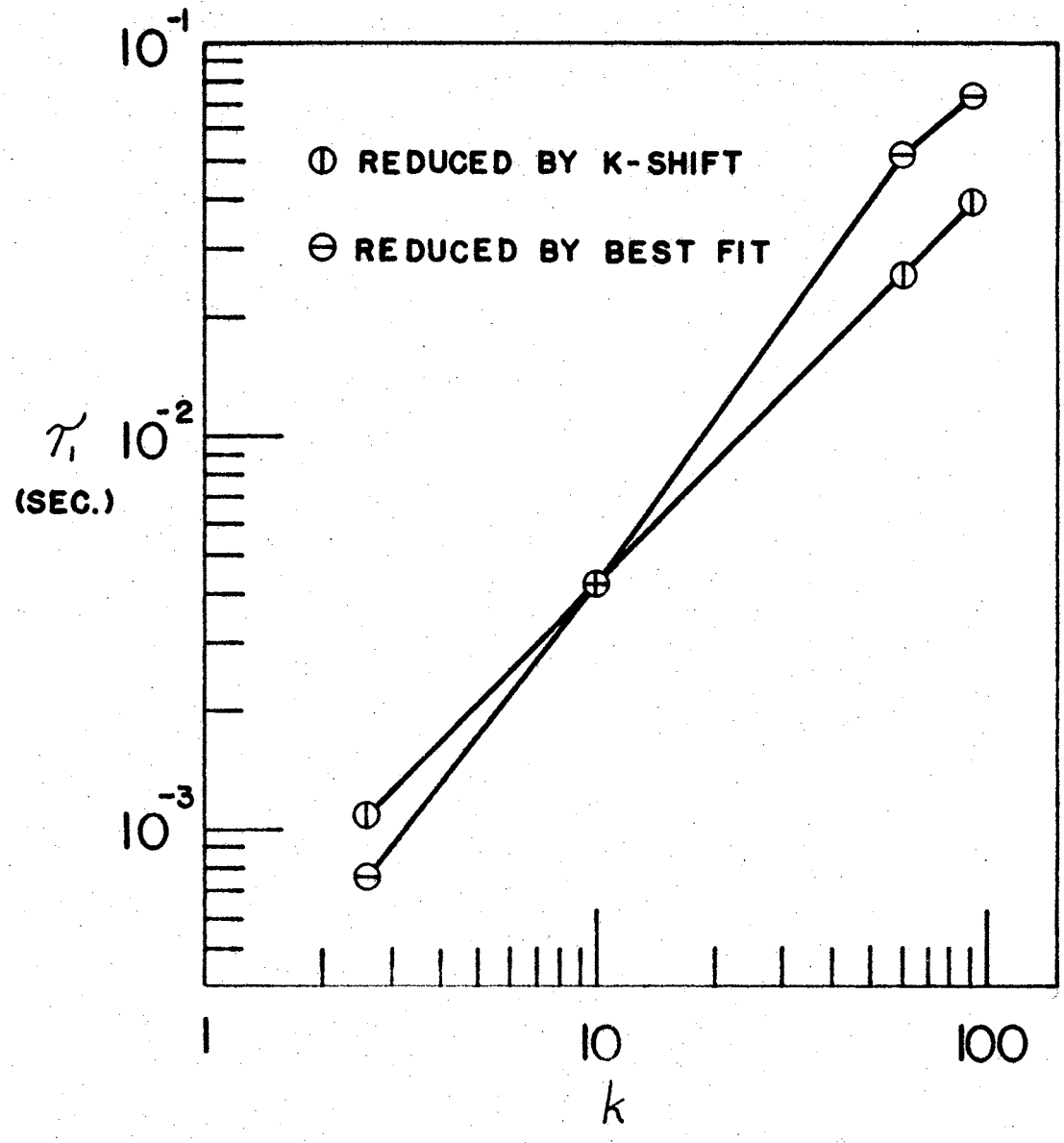
10^{-1}
10^{-2}
10^{-3}
τ_1
(SEC.)
REDUCED BY K-SHIFT
REDUCED BY BEST FIT
1
10
100
k

Baymal in water at 25°C the resulting viscosity increase due to the Baymal was 0.002 poises (34). The concentrations for particular values of k were determined from Figure 7. For the lowest k value used for shear wave propagation data c = 1.06 per cent, k = 2.6 for molecular weight of 480,000, an error of 2.5 per cent may exist in the viscosity due to the presence of the Baymal. This is much less than the variations in the data. As the total solution viscosity increases the possible error will decrease.

The data which determines the curves of Figure 7 was determined using solutions of polyethylene oxide, with the exception of one point. For the .48 x 10^6 molecular weight and a concentration of 4.30 per cent, a solution containing .15 per cent Baymal was used. The fact that this point is consistent with data points determined from pure PEO solutions is another indication of the small effect due to the Baymal.

It should be noted in Figure 11 that the Baymal concentrations for k = 2.6, 61, and 91 was .15 per cent while for k = 10 the Baymal concentration was .30 per cent. No significant irregularities occur in the reduced data due to this difference in Baymal concentration.

In Figure 10 all data was obtained from solutions containing .30 per cent Baymal. When the data from Figure 11 is reduced according to "best fit," Figure 18 is nearly identical to Figure 13. This indicates that the possible error due to the presence of the Baymal is independent of the Baymal concentrations for low concentrations.

From this evaluation one might conclude that the effect of the Baymal on shear wave propagation measurements is very small and that these small rigid birefringent particles are useful indicators when

used with large molecules in solutions where the solution viscosity is at least 50 times that of water. But from Figure 7 it can be seen that a 10 to 20 per cent error can be incurred in determining the intrinsic viscosity if Baymal is present in PEO solutions of low concentration.

Another effect not properly accounted for may be the occurrence of entanglement coupling as described by Ferry and discussed here in Chapter I. This effect increases with molecular weight, and is not included in the a_M function.

B. Conclusions and Suggestions for Further Study

From the extrapolation of steady flow viscosity data the intrinsic viscosities are determined for polyethylene oxide solutions of different molecular weight. The relationship between the intrinsic viscosity and the molecular weight is found to be in reasonable agreement with other available data.

The frequency dependence of the complex viscosity has been determined for solutions containing polyethylene oxide of different molecular weights and in different concentrations. The results of the theoretical model of Zimm are extended to include reduction functions for the effects of variation in both molecular weight and concentration. The reduction function for changing concentrations is based on the assumption that the friction factor not only depends on temperature, but also on polymer concentration. When the resulting reduced curves are compared with the Zimm theoretical relaxation curves, the shapes are nearly identical to the Zimm non-free-draining model curves. Solutions containing a polymer of higher molecular weight (4,000,000) could not be reduced. Thus the reduction scheme is limited in use to relatively

low molecular weights and concentrations.

The relaxation times determined from oscillatory shear data shifted according to the extension of the Zimm theory were a factor of 20 to 30 higher than the relaxation times determined from constant shear measurements. It is possible that this difference is due to a structure formed by the molecules in the solvent. Since the values of τ_1 obtained from oscillatory shear measurements do not agree with the values computed from the steady shear measurements, it appears that values of τ_1 obtained from the Zimm theory may not be proper for the polyethylene oxide solutions studied.

Further study is needed to develop a polymer model which is applicable to solutions of finite concentration since it is difficult to investigate polymers under the conditions prescribed by present dilute solution theories. Extensions of the present dilute solution theories along with experimental data on other polymers could also lead to a new modified model applicable to a particular polymer.

REFERENCES

1. F. E. Bailey, Jr., and R. W. Callard, J. Appl. Poly. Sci. I, 56 (1959)

2. F. E. Bailey, Jr., G. M. Powell, and K. L. Smith, Ind. and Eng. Chem. 50, 8 (1958)

3. F. N. Hill, F. E. Bailey, Jr., and J. T. Fitzpatrick, Ind. and Eng. Chem, 50, 5 (1958)

4. Union Carbide Chemicals, "Polyox" Water-Soluble Resins, # F-40246-C (1964)

5. W. W. Merrill, K. A. Smith, J. Shin, and H. S. Mickley, Trans. Soc. Rheol. 10 (1966)

6. F. Rodriguez, Trans. Soc. Rheol. 10, 169 (1966)

7. J. W. Kinnier and W. A. Reister, Investigation of Low Frequency Properties of Aqueous Polyethylene Oxide Solutions, Thesis, U. S. Naval Postgraduate School (1955)

8. B. H. Zimm, J. Chem. Phys. 24, 269 (1956)

9. W. Haller, Kolloid-Z. 61, 26 (1932)

10. P. Boeder, Z. Physik 75, 258 (1932)

11. W. Kuhn, Z. Physik. Chem. 161A, 427 (1932); Kolloid-Z. 62, 269, (1933)

12. H. G. Jerrard, Chem. Rev. 59, 345 (1959)

13. R. Cerf and H. Scheraga, Chem. Rev. 51, 185 (1952)

14. P. J. Flory, Principles of Polymer Chemistry, Cornell University Press, Ithaca, New York (1953)

15. B. H. Zimm, Rheology, Vol. III, edited by F. R. Eirich, Academic Press, New York, Chapter I (1960)

16. J. D. Ferry, Viscoelastic Properties of Polymers, John Wiley & Sons, Inc., New York (1961)

17. T. W. DeWitt, H. Markovitz, F. J. Padden, Jr., and L. J. Zappas, J. Colloid. Sci. 10, 174 (1955)

18. J. D. Ferry, J. Am. Chem. Soc. 72, 3746 (1950)

19. A. Peterlin, J. Poly. Sci. 12, 45 (1954)

20. J. G. Kirkwood and J. Riseman, J. Chem. Phys. 16, 565 (1948)

21. M. L. Huggins, J. Phys. Chem. 43, 439 (1939)

22. H. A. Kramers, J. Chem. Phys. 14, 415 (1946)

23. J. M. Burgers, Second Report on Viscosity and Plasticity of the Amsterdam Academy of Sciences, Koninklijke Nederlandse Akademie Van Wetenschappen, Verhanddingen afd. Naturkunde, Section 1, 16 (1938)

24. J. G. Kirkwood, Rec. Trav. Chim, Pays-Bas 68, 649 (1949)

25. M. V. Volkenstein, Configurational Statistics of Model Chains in High Polymers, Vol. XVII, Interscience Publishers, New York, 157 (1963)

26. G. B. Thurston and J. L. Schrag, J. Chem. Phys. 45, 3373 (1966)

27. G. B. Thurston, to be published

28. C. W. McGary, Jr., J. Poly. Sci. 46, 51 (1960)

29. G. B. Thurston, Shear Wave Propagation in Birefringent Viscoelastic Liquids of Low Rigidity and Low Viscosity, Technical Report under Contract No. Nonr-2595(03), Stillwater, Oklahoma, Research Foundation of Oklahoma State University (1966)

30. E. I. DuPont de Nemours & Co., Industrial and Biochemicals Department, DuPont Baymal Colloidal Alumina

31. G. B. Thurston and J. L. Schrag, J. Appl. Phys., 35, 144 (1964)

32. J. T. Edsall, Adv. Coll. Sci. 1, 269 (1942)

33. F. E. Bailey, J. L. Kucera, and L. G. Imhof, J. Poly. Sci. 32, 517 (1958)

34. G. B. Thurston, Modern Developments in the Mechanics of Continua, edited by S. Eskinazi, Academic Press, New York (1966)